

CHARACTERIZING LARGE CONDUCTANCE POTASSIUM CHANNELS IN THE
INTRINSIC PRIMARY AFFERENT NEURONS OF MOUSE JEJUNUM

By

Chad Brown, B.Sc. (HONS)

A Thesis

Submitted to the School of Graduate Studies

in Partial Fulfillment of the Requirements

for the Degree

Master of Science

McMaster University

© Copyright by Chad Brown

MASTER OF SCIENCE (2017)

(Medical Sciences)

MCMASTER UNIVERSITY

Hamilton, Ontario

DESCRIPTIVE NOTE

TITLE: Characterizing Large Conductance Potassium Channels in Intrinsic Primary Afferent
Neurons of the Jejunum

AUTHOR: Chad Brown, B.Sc. (Hons) (Brock University)

SUPERVISOR: Dr. Wolfgang Kunze

SUPERVISORY COMMITTEE: Dr. John Bienenstock

Dr. Paul Forsythe

NUMBER OF PAGES: xi, 58

ABSTRACT

Background: The large conductance calcium dependent potassium (BK_{Ca}) channels are expressed in a large variety of cell types including neurons where they modulate excitability and action potential shape. Within the enteric nervous system, stretch-sensitive BK_{Ca} channels are expressed on intrinsic primary afferent neurons (IPANs) where they decrease the neurons' excitability during intestinal contractions. A major determinant of peristalsis is slow excitatory neurotransmission (sEPSPs) within the IPAN to IPAN sensory network, and we wondered whether such transmission might also alter BK_{Ca} channel opening.

Methods: All experiments were performed on longitudinal-muscle myenteric preparations prepared from jejunal segment taken from freshly euthanized adult male Swiss Webster mice. With the myenteric plexus exposed by microdissection, BK_{Ca} channel activity was recorded in cell-attached mode via the patch clamp technique. BK_{Ca} channel activity was recorded before and after presynaptic electrical stimulation, which was designed to evoke postsynaptic sEPSPs. The morphotype was verified by intracellular injection of a marker dye (neurobiotin). In addition, a blocker and opener were used to identify the effects of BK_{Ca} currents on IPAN properties.

Results: Analysis of unitary channel recordings revealed increased BK_{Ca} open probability (NP_o) at fixed trans-patch potentials following sEPSPs. All BK_{Ca} channels were independently voltage sensitive with increased NP_o during patch depolarisation. Analysis of whole-cell experiments also revealed BK_{Ca} channels have a significant effect on the undershoot amplitude of action potentials, and the rate at which IPANs repolarise.

Conclusions: This study demonstrates that sEPSPs within the enteric nervous system modulate the function of BK_{Ca} channels in IPANs adding to the mechanistic understanding of enteric

synaptic transmission and providing a potential target for therapeutic modulation of enteric nervous system excitability.

ACKNOWLEDGEMENTS

I would like to take a moment to thank all the people who helped me throughout my MSc journey.

Firstly, I wish to convey my gratitude to Dr. Wolfgang Kunze for believing in me and providing immense support. Your love for research has been a refreshing experience which has taught me to love whatever I do in the science world. Your drive and motivation have been inspirational while also showing me what it requires to be a world-class researcher. I could not have asked for a better supervisor.

I would like to thank Dr. John Bienenstock for agreeing to be my second supervisor on my committee and providing helpful feedback at times of need. Your open door and welcoming attitude have helped to make my research experience easier while also adding your vast knowledge of gut-brain communication to my thesis. I would also like to thank Dr. Paul Forsythe for agreeing to be my third supervisor on my committee. You helped me to become more confident in presenting by nominating me first in BBI presentations. Your unique outlook on research questions and data as helped me to conceptualize ideas while also giving me the tools to explain data in various ways.

I would like to thank Dr. Yukang Mao, your patience and helpfulness knows no bounds. Your skillset is one of a kind, and sharing the electrophysiology room with you has been a pleasure. Your earnest mentality of making sure I had all the tools I need to continue as a scientist has not gone unnoticed. I would also like to thank Dr. Xuelian Ma, your many years of experience has helped me to become a better patch-clamper. The information that you shared was truly valuable and the time you spent supervising me when I had difficulties was appreciated.

I wish to thank the many individuals in the Brain-Body Institute who made my time there a great experience while also providing a rich learning environment. I would like to thank Dr. Andrew Stanisz for his willingness in ordering chemicals and supplies throughout my Masters. Specifically, from the BBI I would like to thank Dr. Tanvi Javkar, her knowledge and expertise in Microsoft Office shortcuts has greatly helped me with formatting and efficiently writing my thesis.

I owe my deepest gratitude to my wonderful parents, thank you for providing me warm encouragements, love and the best opportunity to get a great education. Your continual support and prayers have sustained me throughout the last two years.

And lastly, thank you Lord for allowing me through all the troubles. You were my biggest strength.

TABLE OF CONTENTS

<u>DESCRIPTIVE NOTE</u>	<u>II</u>
<u>ABSTRACT</u>	<u>III</u>
<u>ACKNOWLEDGEMENTS</u>	<u>V</u>
<u>LIST OF FIGURES AND TABLES</u>	<u>X</u>
<u>LIST OF ABBREVIATIONS</u>	<u>XI</u>
<u>CHAPTER 1: GENERAL INTRODUCTION AND LITERATURE REVIEW</u>	<u>1</u>
1.1 GENERAL DESCRIPTION OF GASTROINTESTINAL PHYSIOLOGY	1
1.2 BIG POTASSIUM (BK_{CA}) CHANNELS - A POTASSIUM CHANNEL SUBGROUP	3
1.3 THE SLO FAMILY OF ION CHANNELS	7
1.4 STRUCTURE OF THE BK_{CA} CHANNEL	8
1.5 BK_{CA} CHANNELS WITHIN THE ENTERIC NERVOUS SYSTEM	8
1.6 MODULATION OF BK_{CA} CHANNELS WORKS VIA INTEGRATED SIGNALLING	9
1.7 ROLE OF BK_{CA} CHANNELS IN THE PATHOPHYSIOLOGY OF DISEASE	12
1.8 HYPOTHESES AND OBJECTIVES OF THESIS	15

CHAPTER 2: EFFECT OF PRE-SYNAPTIC STIMULATION ON BK_{CA} CHANNEL ACTIVITY

AND IPAN EXCITABILITY **15**

PREFACE **15**

2.1 INTRODUCTION **16**

2.2 METHODS **17**

2.2.1 ANIMALS 17

2.2.2 TISSUE PREPARATION 18

2.2.3 ELECTROPHYSIOLOGY SETUP 19

2.2.4 PATCH PIPETTES AND STIMULATING ELECTRODES 21

2.2.5 IN-SITU PATCH CLAMP PREPARATION 22

2.2.6 IN-SITU PATCH CLAMP RECORDING 24

2.2.7 WHOLE-CELL RECORDING 24

2.2.8 MORPHOLOGICAL IDENTIFICATION OF MYENTERIC NEURONS 26

2.2.9 STATISTICAL ANALYSIS 26

2.3 RESULTS **27**

2.4 DISCUSSION **33**

CHAPTER 3: OPENING AND BLOCKING BK_{CA} CHANNELS PHARMACOLOGICALLY TO

DETERMINE THE EFFECTS BK_{CA} CURRENT HAS ON WHOLE-CELL IPAN

ELECTROPHYSIOLOGICAL PARAMETERS **35**

3.1 INTRODUCTION **35**

3.2 METHODS **35**

3.2.1 ANIMALS 35

3.2.2 TISSUE PREPARATION 36

3.2.3	ELECTROPHYSIOLOGY SETUP	37
3.2.4	SHARP ELECTRODE PREPARATION	38
3.2.5	SHARP ELECTRODE RECORDING	38
3.2.6	MORPHOLOGICAL IDENTIFICATION OF MYENTERIC NEURONS	39
3.2.7	STATISTICAL ANALYSIS	40
3.3	RESULTS	41
3.4	DISCUSSION	47
CHAPTER 4: CONCLUSION		49
<hr/>		
4.1	CLINICAL IMPLICATIONS AND TOPICS OF FUTURE RESEARCH	49
4.2	CONCLUSION	50
CHAPTER 5: REFERENCES		52
<hr/>		

LIST OF FIGURES AND TABLES

FIGURE 1. A SCHEMATIC OF THE DIFFERENT LAYERS OF THE GASTROINTESTINAL TRACT.....	2
FIGURE 2. ELECTROPHYSIOLOGY SETUP ILLUSTRATING THE DIFFERENT COMPONENTS ASSOCIATED WITH THE RIG.	20
FIGURE 3. PATCH CLAMP CONFIGURATIONS	23
FIGURE 4. NP_o (THE OPEN PROBABILITY (P_o) X NUMBER OF CHANNELS WITHIN THE PATCH (N))	27
FIGURE 5. BK_{CA} CHANNEL UNITARY CONDUCTANCE.....	28
FIGURE 6. REPRESENTATIVE CELL-ATTACHED PATCH CLAMP CURRENT RECORDING OF THE EFFECT OF PRESYNAPTIC STIMULATION AT 20 HZ.	30
FIGURE 7. EFFECT OF SLOW EPSP ON BK_{CA} CHANNEL NP_o	31
FIGURE 8. DOGIEL TYPE II/AH NEURON SHAPE.	32
FIGURE 9. EFFECTS OF BK_{CA} OPEN PROBABILITY MODULATORS ON RHEOBASE.	41
FIGURE 10. EFFECTS OF BK_{CA} CHANNEL OPEN PROBABILITY MODULATORS ON IPAN INTRINSIC EXCITABILITY.	42
FIGURE 11. EFFECTS OF BK_{CA} OPENER OR BLOCKER ON IPAN RESTING MEMBRANE POTENTIAL.	43
FIGURE 12. EFFECTS OF BK_{CA} CHANNEL OPENER OR BLOCKER ON ACTION POTENTIAL FAST AFTERHYPERPOLARISATION.....	44
FIGURE 13. EFFECTS OF BK_{CA} MODULATORS ON ACTION POTENTIAL MAXIMUM DECAY RATE.	45
TABLE 1. EFFECTS OF BK_{CA} CHANNEL MODULATORS ON WHOLE-CELL PARAMETERS	46

LIST OF ABBREVIATIONS

5-HT	5-hydroxytryptamine
AH cell	After-hyperpolarising cell
AHP	After-hyperpolarisation
BK _{Ca}	Calcium-activated potassium channel of large conductance
Ca ²⁺	Calcium
CGRP	Calcitonin gene-related peptide
CM	Circular muscle
CNS	Central nervous system
CO ₂	Carbon dioxide gas
CTD	C-terminal cytoplasmic domain
DLM	Dorsal longitudinal muscle
ENS	Enteric nervous system
ESRD	End-stage renal disease
fAHP	Fast afterhyperpolarisation
I _A	Transient outward rectifier
IBS	Irritable bowel syndrome
IK _{Ca}	Calcium-activated potassium channel of intermediate conductance
IP ₃	Inositol trisphosphate
IPAN	Intrinsic primary afferent neuron
K ⁺	Potassium
K _{Ca}	Calcium-activated potassium channel
KCl	Potassium chloride
K _v	Voltage-gated potassium channels
LM	Longitudinal muscle
LMMP	Longitudinal muscle myenteric preparation
NK1	Neurokinin receptor 1
NP _o	Number of ion channels x open probability
O ₂	Oxygen gas
OGD	Oxygen/glucose deprivation
P _o	Open probability
RMP	Resting membrane potential
S	Synaptic
sAHP	Slow afterhyperpolarisation
sEPSP	Slow excitatory post-synaptic potential
SK _{Ca}	Calcium-activated potassium channel of small conductance
SP	Sar9-met-O-substance P
5-HT	Serotonin
VSD	Voltage sensing domain

CHAPTER 1: GENERAL INTRODUCTION AND LITERATURE REVIEW

1.1 GENERAL DESCRIPTION OF GASTROINTESTINAL PHYSIOLOGY

The human gastrointestinal tract or gut may be thought of as a hollow tube, which allows substances to transverse through the body, while its main functions are to digest, motile, secrete and absorb nutrients and water. As these substances proceed towards the anal sphincter through the lumen, one of the main catalysts of this process are smooth muscle cells which cause contraction of the intestinal wall, which forces peristaltic movements of the intestinal wall. These peristaltic movements of the gut help to mix and propel nutrients through the gut, while being able to cause segmentation of the gut with each section being able to contract at different forces, frequencies, and durations. The gut is comprised of the esophagus, the stomach, and the small & large intestines, while the liver and pancreas are sometimes also considered apart of the gut. Most digestion and absorption occurs in the small intestine, which is divided into duodenum, jejunum, and ileum. Throughout the gut, layers are superimposed to create the gut wall: the serosa, the longitudinal muscle, the myenteric plexus, the circular muscle, the submucosal plexus, and the mucosa (see figure 1). Within these layers of the gut wall, a network of nerves, muscles, and tissues gives this hollow tube the foundation to be part of the largest sensory nervous system.

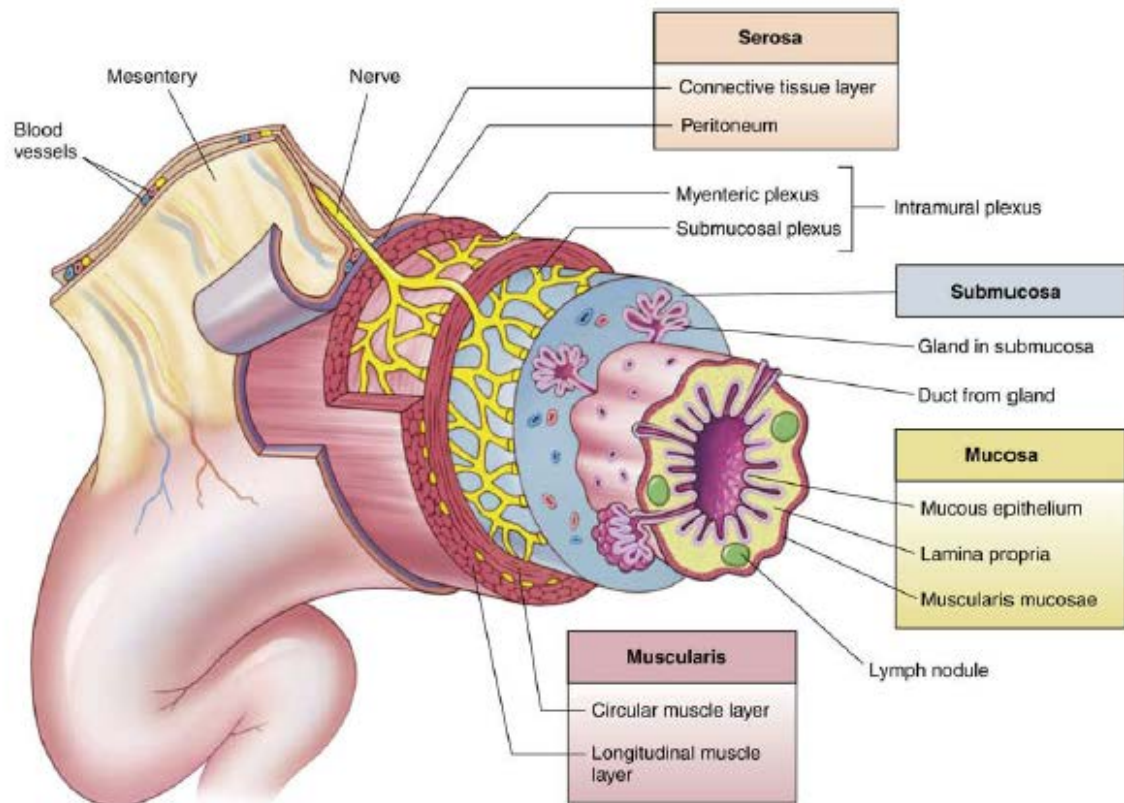


Figure 1. A schematic of the different layers of the gastrointestinal tract.

The enteric nervous system is part of the peripheral nervous system, being a separate division of the autonomic nervous system separate from the sympathetic and parasympathetic divisions. The ENS is the only other nervous system that can function autonomously without input from the central nervous system, however normal digestion requires some communication between the CNS and ENS, with most sympathetic innervation of the gut coming from the vagus nerve, and parasympathetic innervation from either vagus or pelvic nerves. The ENS is located throughout the entire GI tract and forms numerous interconnected networks of plexuses' containing $\approx 500,000,000$ neurons and glial cells in humans (Furness, 2007).

For this thesis, the jejunum is the main section of the gut that is investigated. As stated prior the jejunum connects the duodenum and ileum, with its specialization in absorption via enterocytes. Absorption of small sugars can occur passively while amino acids, peptides, vitamins and larger sugars require active transport. The jejunum is also the area of the gut which has the most innervation whether it is the abundance of sensory neurons or vagal innervation; this makes it an ideal section of the gut to study intrinsic primary afferent neurons.

1.2 BIG POTASSIUM (BK_{Ca}) CHANNELS - A POTASSIUM CHANNEL SUBGROUP

The enteric nervous system (ENS) within the gut of vertebrates such as humans, dogs, pigs, and mice is essential for the coordination of intestinal motility, including propulsive peristalsis, and secretion and absorption. In vertebrates, the ENS is made up of 2 ganglionated plexuses that line the intestine from oesophagus to the internal anal sphincter. The myenteric plexus is located within the external muscular layers between the circular and longitudinal smooth muscle layers; while the submucous plexus is between the mucosal lamina propria and circular smooth muscle (Furness, 2007; Gershon, 1999). The ENS can function independently from spinal or vagal nerves, and comprises a complete nervous system in the sense that it contains sensory, inter- and motor neurons. Chronically disrupted nervous connections between the intestine and central nervous system (CNS) in an in-vivo setting or isolated segments of the intestine ex-vivo, maintain normal reflex function (Ferens et al., 2005; Furness et al., 1995; Kunze & Furness, 1999).

Intrinsic primary afferent neurons (IPANs) are the main chemo- and mechanosensitive neurons within the intestine (Clerc & Furness, 2004; Furness et al., 2004), making up 15 to 25% of the total population of enteric neurons (Kunze & Furness, 1999). They are present in both the myenteric and submucous plexus in all vertebrates from rat to human (Furness, 2007). For smaller

vertebrates such as the mouse, IPANs are present in the myenteric but absent in the submucous plexus (Furness, 2007). For a propagating contractile complex (propagating peristaltic wave) to be initiated, IPANs need to be excited by slow excitatory postsynaptic potentials (sEPSPs) within a network of reciprocally-connected IPANs (Furness et al., 2013; Furness, 2007). Thus, IPANs are critical for normal intestinal functioning, and modulation of their excitability has been suggested to be important in pathology and a potential pharmacological target in therapeutics for functional bowel disorders (Clerc, 2002).

IPANs have a unique shape that distinguishes them from other classes of neurons in the enteric nervous system. They have a large oval soma (cell body) and several long processes (neurites) which innervate other IPANs, and inter- and motor neurons lying in the same ganglion or other ganglia. All IPANs have neurites with long circumferentially directed projections, and a small percentage (<6%) also have a few shorter neurites projecting either orally or anally (Bornstein, Furness, & Kunze, 1994; Hendriks, Bornstein, & Furness, 1990; Kunze & Furness, 1999; Kunze, Furness, & Bornstein, 1993). This characteristic IPAN shape has been named “Dogiel type II” after the researcher who first described their morphology (Dogiel, 1899; Furness et al., 1998). In contrast, inter- or motor neurons are unipolar with a single axon and either a smooth soma or one possessing several short dendrites.

IPANs are mechanosensitive; their neurites generate action potentials when they are stretched and their somatic action potential firing is inhibited when the somata are compressed (Kunze et al., 2000; Kunze, Furness, Bertrand, & Bornstein, 1998). They also provide 90% or more of sensory neuropeptide-containing innervation of the mucosal epithelium which lines the intestinal lumen (Ekblad et al., 1987; Furness & Costa, 1984). In the guinea pig, for which detailed

measurements have been made, each enteric IPAN innervates 80-120 villi (Kunze & Furness, 1999).

IPANs also have a unique electrophysiological signature that differentiates them from other types of neurons in the ENS. They are in many respects similar to C δ dorsal root ganglia neurons. The upstroke of the action potential is generated by a mixture of sodium and calcium conductances with the calcium current producing a hump on the repolarising phase of the action potential. The repolarising phase continues below the resting membrane potential to produce an undershoot or fast afterhyperpolarisation (fAHP) which is generated by a mixture of conductances including the K⁺ delayed rectifier, the A current or transient outward rectifier (I_A), and opening of large conductance calcium-activated K⁺ channels (BK_{Ca}) (Furness et al., 1998; Furness et al., 1996; Rugiero et al., 2002). The inward calcium current during the action potential not only activates I_{BK} but also a delay slow afterhyperpolarising potential (sAHP). The sAHP is a major determinant of IPAN excitability and was first described by David Hirst (Hirst et al., 1972) and Allan North (North, 1973). The presence of post-action potential sAHP in IPANs led Hirst to name them “AH cells” so that IPAN, Dogiel type II neuron and AH cell refer to the same neuron. Inter- or motor neurons generally lack an sAHP and receive fast excitatory postsynaptic potentials, which is why Hirst named them “S cells” (S for synaptic); S cells, like AH cells, receive sEPSPs from presynaptic AH cells (Gwynne & Bornstein, 2007; Kunze et al., 1993). The sEPSP increases IPAN excitability by decreasing the open probability of the IK_{Ca} channel (Mao, Wang, & Kunze, 2006; Wood & Kirchgessner, 2004). The ion channels whose opening generates the sAHP have been identified as being of the intermediate conductance Ca²⁺-dependent K⁺ (IK_{Ca}) type (Furness et al., 1998; Mao et al., 2006) and have been extensively studied (Mao et al., 2006; Neylon et al., 2004; Neylon, Fowler, & Furness, 2006; Nguyen et al., 2005; Nguyen et al., 2007; Vogalis, Furness, &

Kunze, 2001; Vogalis, Harvey, & Furness, 2003). As mentioned earlier, the inward Ca^{2+} current during the IPAN action potential increases intracellular Ca^{2+} thus opening IK_{Ca} channels. BK_{Ca} channels, whose opening contributes to the fast afterhyperpolarisation (fAHP), are another important Ca^{2+} -dependent K^{+} channel is opened by the rise in intracellular Ca^{2+} concentration. Several properties suggest that BK_{Ca} channels also make an important contribution to the intrinsic excitability of IPANs. IPAN BK_{Ca} channels have a non-zero open probability at resting membrane potential and because they are steeply voltage-dependent their open probability will increase even with small membrane depolarisations of only 10 mV (Kunze et al., 2000). The increased BK_{Ca} open probability increases total membrane conductance and hyperpolarises the membrane, both factors work to decrease IPAN intrinsic excitability. AH cell BK_{Ca} channels have a large unitary conductance of about 200 pS (Kunze et al., 2000) (versus about 30-70 pS for IK_{Ca} channels), so fewer BK_{Ca} than IK_{Ca} channels need to open (or close) to have a significant effect on whole cell IPAN membrane potential. In addition, IPAN, but not S cell, BK_{Ca} channels are mechanosensitive, altering their open probability when the neuron soma is compressed or stretched (Kunze et al., 2000). These combined properties of BK_{Ca} channels suggest that they would also have an important role in the control of IPAN excitability and therefore intestinal motility.

Given the importance of sEPSPs for enteric nervous system and intestinal motility normal functioning, and the link between intracellular Ca^{2+} levels and IK_{Ca} and BK_{Ca} activity, an interesting question to ask is: do sEPSPs modulate BK_{Ca} open probability? The discovery that IPAN intracellular free Ca^{2+} concentrations are increased during the sEPSP (Hillsley, Kenyon, & Smith, 2001) suggests that Ca^{2+} concentrations can also modulate BK_{Ca} channel opening.

Potassium (K^{+}) channels are the largest and most diverse family of ion channels, they have a reversal potential (equilibrium potential) that is near or more negative to the resting membrane

potentials (RMP) of typical cells. K^+ channels have an important role in the overall excitability, background activity, and firing patterns of neurons and secretory endocrine cells, along with roles in determining the shape and duration of action potentials. BK_{Ca} channels are voltage-gated K^+ channels that integrate changes in intracellular calcium and membrane potential. In addition, unlike most BK_{Ca} neuronal channels BK_{Ca} channels expressed on IPANs also integrate stretch or pressure with membrane voltage and Ca^{2+} sensitivity.

1.3 THE SLO FAMILY OF ION CHANNELS

Within the Slo family, there are four genes that encode four different α -subunits. *Slo1* (also referred to as maxi-K, BK_{Ca} channels), *Slo2.1* (slick), *Slo2.2* (slack), and *Slo3* are the various genes encoding the α -subunits that form the homotetrameric structure required for the pore of the channels. These genes differ greatly in their individual gating properties and structure and were first discovered in *Drosophila*. Initial BK_{Ca} channel experiments were performed in cats, where Ca^{2+} was injected into motoneurons resulting in an increase in membrane conductance, and a decrease in cellular excitability, suggesting a calcium-dependent K^+ current at work (Contreras et al., 2013; Krnjević & Lisiewicz, 1972). BK_{Ca} channel calcium-dependence was later investigated in the dorsal longitudinal muscles (DLMs) of a *Drosophila* mutant, the phenotype named 'slowpoke', expressed a lack of locomotion. Voltage-clamp and current-clamp experiments revealed ablation of the calcium-dependent component of the outward K^+ current, which provided evidence that this *slowpoke* allele was important for channel (pore) formation (Elkins, 1986; Salkoff et al., 2006). The *slowpoke* allele was later isolated and cloned and shown to produce BK_{Ca} channels, and to have molecular characteristics that were conserved across mammals (Adelman et al., 1992; Atkinson, Robertson, & Ganetzky, 1991; Butler, Tsunoda, McCobb, Wei, & Salkoff,

1993; Contreras et al., 2013; Elkins, 1986). Supplementary findings have since highlighted the importance of BK_{Ca} channels in neurotransmitter release from presynaptic terminals, its function as a negative feedback mechanism for depolarisation and the highly regulated intracellular Ca²⁺ concentration (Bartschat & Blaustein, 1985; Contreras et al., 2013; Orio, Rojas, Ferreira, & Latorre, 2002; Salkoff et al., 2006).

1.4 STRUCTURE OF THE BK_{Ca} CHANNEL

BK_{Ca} channels are ubiquitous throughout mammalian physiology particularly within the nervous system. Functionally, BK_{Ca} channels may have different properties due to alternative splicing, but their structure remains consistent. BK_{Ca} channels structure resembles voltage-gated K⁺ (K_v) channels due to a homotetrameric arrangement of 4 pore-forming α -subunits, but differ in regards to the large C-terminal cytoplasmic domain (CTD) and an additional transmembrane segment (S0) for BK_{Ca} and Slo3 channels (Contreras et al., 2013; Schreiber et al., 1998; Wallner, Meera, & Toro, 1996). Each α -subunit within the BK_{Ca} channels contains 7 transmembrane segments S0-S6, with S4 having a crucial role in voltage sensing. Ca²⁺ binding sites have been identified within the CTD, which are involved in ion permeation, gating, and modulation of the channel through secondary messenger factors (Contreras et al., 2013; Quirk & Reinhart, 2001).

1.5 BK_{Ca} CHANNELS WITHIN THE ENTERIC NERVOUS SYSTEM

BK_{Ca} channels contained on IPANs are one of the great integrators of stimuli in physiology. IPAN BK_{Ca} channels are mechanosensitive. Although mechanosensitive neurons were first recorded by (Eyzaguirre & Kuffler, 1955; Katz, 1950), mechanosensitive neurons within intestinal walls were first identified by (Kunze & Furness, 1999; Kunze et al., 1998). Cell-attached patch-

clamp recordings of mechanosensitive BK_{Ca} channels determined that positive pressure doubled the open probability (P_o) while negative pressure did not. Increasing BK_{Ca} open probability by pressing on the IPAN reduced spontaneous action potential discharge (Kunze et al., 2000). These experiments were also the first to show repeated pressure briefly opened previously silent BK_{Ca} channels and primed the BK_{Ca} channels for larger increases in P_o of guinea pig duodenum.

1.6 MODULATION OF BK_{Ca} CHANNELS WORKS VIA INTEGRATED SIGNALLING

Voltage-sensitive properties of BK_{Ca} channels are one determinant of P_o . P_o is a value between 0 and 1 based on the ion channel's opening characteristics which refers to the proportion of time that the channel spends in the open configuration. Substantial evidence for a voltage sensor came from experiments that measured gating currents in the absence of intracellular Ca²⁺ (Horrigan & Aldrich, 1999; Horrigan & Aldrich, 2002; Stefani et al., 1997). The specific mechanism and molecular interactions between the voltage sensing domain (VSD) and other domains/ subunits is still under investigation and is strongly dependent on mathematical models (Li & Yan, 2016). Auxiliary subunits particularly, the β subunit have been reported to modulate voltage dependence and kinetics of the BK α subunit (Contreras et al., 2013; Li & Yan, 2016). Kunze et al., 2000 examined BK_{Ca} channels of IPANs and their response to trans-patch potentials. It was reported that hyperpolarising voltage steps decreased channel openings but increased the amplitude of the current, while depolarising voltage steps increased channel activity and decreased the amplitude of the current. Voltage dependency was illustrated by a P_o –V graph, a clear dependency was shown by a sigmoidal curve showing increased voltage correlates to increased P_o .

Mechanosensitivity Channels that respond to pressure/and or stretch pertain to sensory functions of the body, where muscle composition and movement is abundant. One such place is under the intestinal epithelium. IPANs were excited by mechanical distortion of their processes and inhibited by mechanical force to the somata in guinea pigs (Kunze et al., 2000). Positive and negative pressure were applied via intrapipette pressure. Positive pressure increased the open probability of BK_{Ca} channels by 2-fold, but there was little effect when negative pressure was applied (Kunze et al., 2000).

Calcium sensitivity of myenteric BK_{Ca} channels is an area that has not been thoroughly investigated. In low [Ca²⁺] the calcium-dependent hump was reported to be abolished on the falling phase of the action potential of IPANs (Kunze et al., 2000). In addition, pressure sensitivity persisted even in low [Ca²⁺] which can infer that BK_{Ca} channels are both calcium sensitive and mechanosensitive (Kunze et al., 2000).

Calcitonin gene-related peptide (CGRP) is a peptide produced in both the central and peripheral nervous systems with physiological functions in respiratory, immune and the gastrointestinal systems. Within the submucosa slow excitatory post-synaptic potentials (sEPSPs) are necessary for excitation to spread, and are the determining factor in initiating excitation of cholinergic/CGRP containing primary afferent neurons. Antagonizing CGRP with human calcitonin gene-related peptide (hCGRP₈₋₃₇) resulted in blockage of sEPSPs (Pan & Gershon, 2000). It was also reported that hCGRP₈₋₃₇ reduced excitation within the submucosal plexus (Pan & Gershon, 2000). This provided some of the first evidence that CGRP is necessary for sEPSPs which is in part responsible for the spread of excitation. It was observed that a subset of neurons still exhibited sEPEPs in the presence of hCGRP₈₋₃₇, which supports the hypothesis of there being neurons that use CGRP as a co-transmitter with acetylcholine (Pan & Gershon, 2000). Lastly,

experiments that used scopolamine, a muscarinic antagonist, and NK₁₋₃ receptor antagonists to inhibit responses to mucosal application of serotonin (5-HT) were not adequate to block the responses (Pan & Gershon, 2000). Further investigation of CGRP in other animal models is required with respect to function and distribution within the ENS of other neuronally populated plexi such as the myenteric plexus.

Oxytocin is a hormone and a neuropeptide that is ubiquitous throughout mammalian physiology, with functions varying from reducing pain in labour to effecting social behaviour. Oxytocin is contained within the paraventricular nuclei of the hypothalamus, which is then secreted into the bloodstream from the posterior pituitary gland nerve endings (Nicholls et al., 2012). Investigation of oxytocin was primarily performed in the CNS until recently Che et al., 2012 reported that oxytocin and its receptor had a prominent function in the ENS. Their major claim was that oxytocin hyperpolarised cultured myenteric intrinsic primary afferent neurons of the duodenum by opening BK_{Ca} channels through the IP₃ pathway. This leaves a gap in the understanding of oxytocin and questions thus arise as to what oxytocin does in other intestinal regions such as the jejunum.

Sar9-met-O-substance P (SP) an agonistic neurotransmitter for neurokinin receptor 1 (NK1) was first discovered to be localized within primary afferent neurons of rats (Author et al., 1975). SP is an ubiquitous neuropeptide which acts a neuromodulator with various functions such as stimulating cell growth (Katsanos et al., 2008), an inflammatory peptide released from primary afferents that respond to painful stimulation or injury (Donkin et al., 2007; Hunt et al., 1998), and a vasodilation molecule (Bossaller et al., 1992). Within the dorsal horn of the spinal cord substance P has a promoting effect on central hyperexcitability and increased sensitivity to pain following intense peripheral stimulation (Hunt et al., 1998). This opposes the main function of BK_{Ca}

channels and potassium channels as a whole, which are important for restoring membrane potential, and preventing hyperexcitability. Experiments observing the relationship between NK1R/substance P agonist and the BK_{Ca} channel have not been investigated within the gut. This could provide a window of opportunity for therapeutic targets for understanding neurogenic pain or bowel diseases where hyperexcitability is the pathological mechanism.

1.7 ROLE OF BK_{Ca} CHANNELS IN THE PATHOPHYSIOLOGY OF DISEASE

BK_{Ca} channels have various functions throughout the body, and deficits in channel formation can lead to a vast array of pathology including increased arterial pressure and vascular tone, tremors, ataxia and hearing loss (Rüttiger et al., 2004; Sausbier et al., 2004). There is a body of literature describing the variety of physiological outcomes that arise due to BK_{Ca} channel dysfunction, and here we briefly summarize these findings.

Within the CNS BK_{Ca} channels have been investigated within the brain. The following are the major findings of the deficits within this system. Reduced mRNA coding for the KCNMA1 gene has been shown to reduce BK_{Ca} channel activity, which is observed in patients with autism and mental retardation (Laumonnier et al., 2006). It has also been reported that mice lacking BK_{Ca} channels are observed to have cerebellar dysfunction, such as abnormal eye-blink reflex, motor coordination and reduction in activity of cerebellar Purkinje neurons which generate the output of the cerebellar cortex (Sausbier et al., 2004). BK_{Ca} channels have been implicated in having a role in early post-ischemic phase and oxygen/glucose deprivation (OGD). BK_{Ca} channel blockers, paxilline and iberiotoxin were used during and after OGD-induced cell death. Increased cell death of CA1 and CA3 was observed due to the regulatory role of presynaptic BK_{Ca} channels on glutamate release (Rundén-Pran et al., 2002). It has been discovered that BK_{Ca} channels also have

an important role in hearing. The lack of pore formation via the α -subunit within the mammalian cochlea did not have an effect on congenital hearing loss. Rather mild progressive high-frequency loss was observed (Rüttiger et al., 2004). Deletion of the α -subunit trumped the normal phenotypes of outer hair cells and inner hair cells, which provided more evidence that BK_{Ca} channels, specifically the α -subunit are essential for hearing loss in outer hair cell degeneration (Rüttiger et al., 2004). In a study by Typit et al., 2013, the findings mentioned before, specifically the deficits in autism, mental retardation, and hearing loss were confirmed. In addition to those findings, learning and memory were observed to be affected in BK_{Ca} channel-deficient mice, by affecting the rate of learning tasks such as the Morris water maze. Interestingly this group did note that working memory and spatial reference memory were not affected, but more work is required to fully understand the BK_{Ca} channel's role. Further investigation of BK_{Ca} channels has also discovered that downregulation of this ion channel has implications in the pathogenesis of genetic epilepsy. Pacheco Otorola et al., 2008 further investigated the BK_{Ca} channels functional role in a pilocarpine temporal lobe model of epilepsy. Findings indicated BK_{Ca} channel expression was down-regulated in the dentate gyrus of the hippocampus pilocarpine-treated epileptic rats. Also, rats experiencing more seizures or longer post-status epilepticus survival period displayed a greater decline in BK_{Ca} channel expression.

Within recent years therapeutic investigations of the role of BK_{Ca} channels in chronic pain has been an expanding area. Chronic pain is associated with abnormal excitability in the somatosensory system (Tsantoulas & McMahon, 2014). Electrogenesis at the site of injury, mid-nerve, or the dorsal root ganglia cell body can occur spontaneously, which increases the likelihood of increased neuronal excitability and action potential generation and propagation (Tsantoulas & McMahon, 2014). Zhang, Gopalakrishnan, & Shieh, 2003 reported that NS-1619 (BK_{Ca} channel

opener), suppressed action potential firing, and antagonized the hyperexcitability evoked by A-channel block. This effect was sensitive to iberotoxin which prolonged the duration of the action potential and increased the firing frequency of afferent neurons between L6 and S1 of adult rats, which indicated the effect was mediated by BK_{Ca} channels (Tsantoulas & McMahan, 2014; Zhang, Gopalakrishnam, & Shieh, 2003). Ablation of BK_{Ca} channels has also been associated with enhanced inflammatory pain but normal neuropathic and acute nociceptive pain behaviour (Lu et al., 2014; Tsantoulas & McMahan, 2014).

Atypical electrophysiological behaviour or expression of BK_{Ca} channels fundamentally changes the homeostasis of the electrochemical gradient, which in turn can lead to pathology such as Hypokalaemia (low K⁺ in the blood). Many enteric pathogens elicit watery diarrhoea leading to an excessive K⁺ loss in stool (Sandle & Hunter, 2010). Acute cholera and *Clostridium difficile* colitis follow the same mechanism of activation of cAMP-dependant BK_{Ca} channels underlying colonic K⁺ secretion that accompanies the marked small intestinal secretion of Cl⁻ and water (Butler et al., 1986; Guerrant et al., 1973; Lauritsen et al., 1988; McDonel, 1974; Sandle & Hunter, 2010). It has been recently discovered that apical BK_{Ca} channels are located in surface cells and cells in the upper 20% of human colon crypts (Sandle & Hunter, 2010). This, alongside the additional finding of an absence of colonic K⁺ secretion in BK_{Ca}-knockout mice suggests that these BK_{Ca} channels are the only exit pathway for luminal K⁺ ions (Sandle & Hunter, 2010; Sausbier et al., 2006). Lastly, overexpression of BK_{Ca} channels on surface colon epithelial cells and crypt cells was found in end-stage renal disease (ESRD) in addition to an increase in the apical K⁺ permeability of the large intestinal epithelium which suggested the threefold increase of basal K⁺ secretion is linked (Mathialahan et al., 2005).

1.8 HYPOTHESES AND OBJECTIVES OF THESIS

The sEPSP decreases $I_{K_{Ca}}$ open probability (P_o) in IPANs, this causes a decrease in the post action potential sAHP. In the literature review I argued that since the open probability of BK_{Ca} channels is also dependent on intracellular Ca^{2+} concentration, the sEPSP would similarly decrease BK_{Ca} P_o . I therefore hypothesize that neurotransmission via sEPSP between IPANs reduces myenteric BK_{Ca} channel opening. This hypothesis will be tested by single-channel and whole-cell recording from myenteric jejunal IPANs.

Objective 1 – determine what effect sEPSPs have on BK_{Ca} channels by evoking sEPSPs electrically at pre-synaptic intermodal strands, and using in-situ patch clamp of the soma to determine the P_o .

Objective 2 – determine how excitability of IPANs is altered when BK_{Ca} P_o is increased or decreased using BK_{Ca} channel pharmacological blockers or openers.

CHAPTER 2: EFFECT OF PRE-SYNAPTIC STIMULATION ON BK_{Ca} CHANNEL ACTIVITY AND IPAN EXCITABILITY

PREFACE

The main aim of these experiments was to determine whether the slow (metabotropic) excitatory synaptic input to IPANs alters the probability of being open (P_o) of BK_{Ca} channels and if it did so, in which direction. These experiments were most directly done by single channel recording in cell-attached mode because BK_{Ca} channel activity is recorded in real-time before during and after activation of the sEPSP. In contrast, during whole-cell recording, BK_{Ca} channel current can only be measured after applying a BK_{Ca} channel blocker such as paxilline and then subtracting the currents before and after applying the blockade. The duration of the sEPSP ranges

from several seconds to 2 min and during this period rises to an initial maximum and then decays. Washing in a BK_{Ca} channel blocker to achieve close to 100% blockade may take up to 15 min. These considerations made it difficult to use whole-cell recording to study BK_{Ca} channel currents during the sEPSP.

2.1 Introduction

There have been few patch clamp recordings from in situ enteric neurons despite the advantages conferred by patch clamp method, such as the ability to record unitary ion channel currents. The advantage of in situ recording include the preservation of synaptic connections between neurons within the ENS. This allows us to record the effects of presynaptic stimulation on ion channels on the postsynaptic neuron. Since ion channels could be potential therapeutic targets themselves, or the activity may be modulated by coupled ionotropic or metabotropic receptors, the ability to record postsynaptic responses of single ion channels may have important translational relevance.

The ENS presents several difficulties with respect to in situ patch clamp recording. Firstly, the myenteric plexus is situated in the external muscular coat between the circular and longitudinal muscle layers preventing access to the neurons with a patch pipette. This was solved by making a classical longitudinal muscle myenteric plexus (LMMP) preparation for which the mucosa, submucosa and circular muscle are carefully dissected away with forceps down the midline of the preparation. All excess layers were then peeled back and pinned and finally excised until the myenteric plexus was exposed and resting on the longitudinal muscle beneath. Second, neurons of the myenteric plexus are covered by glial cells and adherent connective tissue. This prevents access of the patch pipette to clean areas of neuronal membrane and requires specialized cleaning techniques to expose part of the neuronal membrane whilst leaving synaptic connections intact.

Third, smooth muscle on which the myenteric plexus rests has intrinsic contractile activity which needs to be minimised (although it cannot be completely abolished) before successful patch clamp seals and recordings can be obtained. This problem is to some extent overcome by applying a L-calcium channel blocker to the Krebs saline buffer to the solution perfusing the LMMP. Because L-calcium currents are functional on the smooth muscle but not enteric neurons the blocker is thought to have minimal effects on the physiology of the latter.

The technique of in situ myenteric neuron patch clamping was first used in the guinea pig small intestine and was later adapted for mouse small intestine (Kunze et al., 1993; Mao et al., 2006). These previous efforts used exposure to protease type XIV to soften the connective tissue which was then removed using a fine sable brush hair. For the present experiments, we have modified and simplified the protocol by substituting 0.4 mg/ml pronase (Roche, <http://www.rochecanada.com>) and 0.5mg/ml collagenase type I (Worthington, <http://www.worthington-biochem.com>) (Kunze et al., 2009) for the protease which obviated the need for manual cleaning with the hair. Nevertheless, this patch clamp recording method is technically demanding and requires a high degree of attention to detail.

2.2 Methods

2.2.1 Animals

Adult male Swiss Webster (SW) mice (20–30 g, ~3–4 months old) were procured from Charles River Laboratories (Wilmington, MA, USA). After >1-week acclimatization in the St Joseph's animal facility, mice were transported to the laboratory and killed by cervical dislocation. All ensuing procedures were ex-vivo. All animal protocols were covered by the McMaster animal utilisation protocol #160830.

2.2.2 Tissue preparation

After the mouse was sacrificed, it was placed ventral side up on a cork board and stretched out using 22-gauge syringe needles to impale fore and hind paws. The skin was opened by a vertical midline abdominal incision and retracted to expose the underlying muscle. The abdominal skeletal muscle coat was opened with another vertical midline incision using surgical scissors and retracted to expose the viscera. A 3-4 cm segment of middle jejunum was excised, taking care not to unduly stretch the attached mesentery and vessels nor to touch or stretch the segment. The segment was freed from the adherent mesentery by cutting with surgical scissors and placed in a recording chamber made using a polystyrene petri dish (Falcon 1006, 50 mm×9 mm, Becton Dickinson, NJ, USA). The bottom of the dish was lined 2 mm deep with cured silicone elastomer (Sylgard®, Dow Corning, MI, USA) and filled with cold Krebs saline (composition in mM: NaCl 118.1, KCl 4.8, NaHCO₃ 25, NaH₂PO₄ 1.0, MgSO₄ 1.2, glucose 11.1, and CaCl₂ 2.5) to which 3 μM nifedipine (Sigma-Aldrich, Oakville, CA) and 10 μM scopolamine (Sigma-Aldrich, Oakville, CA) had been added. The saline was oxygenated and pH buffered by being continuously gassed with carbogen (95% O₂, 5% CO₂).

The following dissection was carried out using a Nikon zoom stereomicroscope (Nikon Instruments Inc, <https://www.nikoninstruments.com>) with 40 × magnification. The mesenteric attachment was dissected away using fine surgical scissors and the jejunal segment opened by cutting in the oral to anal direction along the line of mesenteric attachment. The open segment was pinned flat with mucosa uppermost using 2 cm long insect pins at each corner with the oral edge uppermost in the dish. Using fine dissection forceps and starting at the anal end the mucosa and submucosa were gently lifted off the underlying circular muscle and progressively teased away until it was entirely removed. Now, the tissue was re-pinned and stretched using 40 μm diameter

tungsten wire pins to anchor the edges. The circular muscle was then carefully removed by microdissection taking care to minimise damage to the underlying myenteric plexus. When 50% or more of the circular muscle had been removed the tissue in the recording chamber was allowed to rest by being placed in a glass beaker filled with 1 L oxygenated Krebs saline plus nicardipine.

2.2.3 Electrophysiology Setup

The tissue and recording chamber were placed onto the stage of a Nikon eclipse inverted microscope (Nikon Instruments Inc, <https://www.nikoninstruments.com>) and the tissue perfused (4 mL/min) with prewarmed (35°C) oxygenated Krebs saline and nicardipine/scopolamine driven by a VWR heated peristaltic pump (VWR, <https://us.vwr.com>). A grounding wire consisting of a chlorided 2 cm long silver wire was placed into the Krebs saline in the recording chamber. The return was connected to the common earth input of the recording amplifier. Enzymes or drugs were delivered onto the tissue via a 200-300 µm diameter glass pipette by gravity feed from a 10 mL

plastic syringe positioned 20 cm above recording chamber.

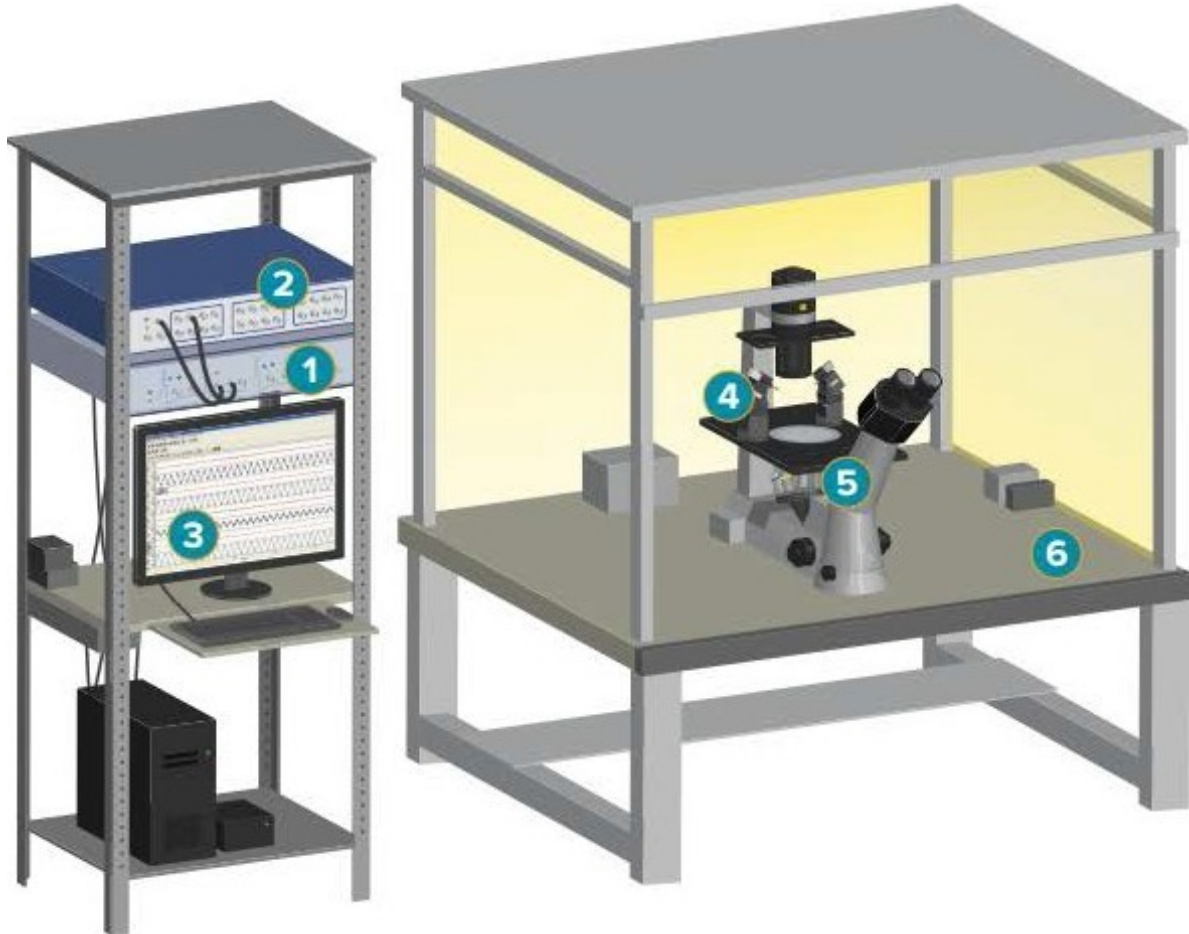


Figure 2. Electrophysiology setup illustrating the different components associated with the rig. Reprinted from Molecular Devices. 2017. Retrieved from <https://www.moleculardevices.com/systems/axon-conventional-patch-clamp>. Reprinted with permission.

The microscope was mounted on a TMC vibration isolation table (Technical Manufacturing Corporation, <http://www.techmfg.com>) and the whole surrounded by a grounded Faraday cage to isolate them from electric fields. The recording electrode consisted of a chloride silver wire inserted into a patch pipette holder which was connected to an Axon Instruments MultiClamp 700B computer amplifier (Molecular Devices, Sunnyvale, CA, USA) which could record voltage signals in current clamp mode or currents in voltage clamp mode. The amplified

signals were fed into an Axon Instruments Digidata 1550B digitiser (Molecular Devices, Sunnyvale, CA, USA) which converted the analog signals to digital ones which could be displayed in real-time on a PC computer running pClamp 10 (Axon Instruments) software and was stored on computer hard drive and USB for post-hoc analysis. Electrical signals were acquired at 20 kHz with a Bessel filter applied at 2 kHz.

2.2.4 Patch pipettes and stimulating electrodes

Patch pipettes were manufactured from thick-walled borosilicate glass tubing (ID = 0.86 mm, OD = 1.5 mm, BF150-86-10, Sutter instruments) using a Brown-Flaming P-97 programmable pipette puller (Sutter instruments). The patch pipette solution used to fill the pipette was a K⁺-rich solution (composition in mM: KMeSO₄ 115, NaCl 9, CaCl₂ 0.09, MgCl₂ 1.0, HEPES 10, Na₃GTP 0.2, and BAPTA.K₄ 0.2 with 1% Neurobiotin tracer (Vector Laboratories, <https://vectorlabs.com>), and 14 mM KOH added to bring the pH to 7.3). This solution is designed to record K⁺ unitary currents during cell-attached recording, and to preserve intracellular Ca²⁺-dependent currents during whole-cell recording (Mao et al., 2006). The solution was freshly made on the day of the experiment and filtered through a 0.2 um pore 4 mm diameter filter (MicroFil, WPI) before use. The parameters of the pipette puller were adjusted so that the patch pipettes had resistance of 8 to 10 MΩ when the tip was placed within Krebs saline. Each pipette was filled just before use and inserted into the patch pipette holder of the amplifier head stage.

Electrical stimuli were delivered to interganglionic connectives using tungsten wires etched to 10–20 μm in tip diameter that were insulated except at the tip. Slow EPSPs were evoked by 20 Hz trains of 0.1 ms pulses at an intensity of 0.1 - 0.5 mA for 1 s delivered by an ISO-flex stimulus isolation unit (AMPI, <http://www.ampi.co.il/>) controlled by a Master 8 gated pulse generator (AMPI) under computer control from within pClamp running on the PC. Intra- patch

pipette pressure was measured using an in-house pressure transducer whose pressure input was connected to a parallel port of the recording pipette holder and whose analog output was fed into the digitiser, whose digital output, in turn, was supplied to the computer and displayed as one of the recording channels displayed within the pClamp software.

2.2.5 In-situ patch clamp preparation

Initially using low-power (50-100x) and then higher power (400x) a myenteric plexus ganglion was selected if it contained what appeared to be healthy neurons. We attempted to select IPANs for patching which had Dogiel type II morphology. To prevent the recording pipette tip being blocked by debris floating on the surface of the extracellular solution or in the solution, 50 hPa positive pressure was applied to the pipette before its tip entered the Krebs saline filling the recording chamber. After the patch pipette entered the saline in the recording chamber, any DC and capacitive offsets recorded by the amplifier was zeroed using the amplifier. The interface of 2 solutions (intracellular-patch pipette versus Krebs saline) produces a liquid junction potential. After zeroing the electrode DC offset and capacitative transients in the intracellular solution, a shift of 4-5 mV was seen when the pipette was dipped into Krebs saline. This liquid junction potential would have affected potentials recorded in cell-attached as well as the whole-cell configuration if the tip potential was not 'zeroed' to offset this liquid junction potential.

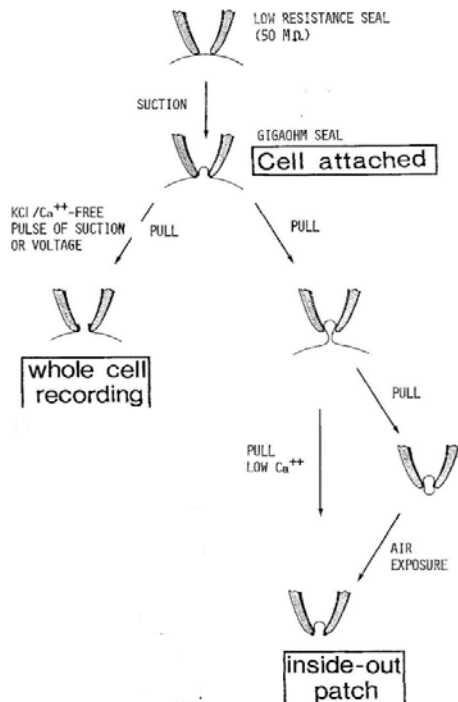


Figure 3. Patch clamp configurations, adapted from Hamill et al. Improved patch clamp techniques for high resolution current recordings from cells and cell-free membrane patches. Pflugers Arch 1981;391:85–100.

While in the solution the amplifier was in voltage clamp mode and repeated (10 Hz) voltage steps (-5 mV) were applied, the resulting current pulses were used to measure the ohmic pipette resistance and to monitor seal formation using the “seal-test” function in pClamp. If the pipette resistance was not 6-14 MΩ, it was discarded and the new pipette substituted. 50 hPa pressure was maintained until the pipette tip approached the selected neuron when the intrapipette pressure was reduced to approximately 10 hPa and the

tip gently pushed against the neuron membrane visualised as a slight dimpling of the neuron surface. The patch pipette was then pushed further against the membrane until the current pulse generated by the

voltage steps had decreased by 10-30% of its original amplitude; this indicates a further decrease in the resistance (seal resistance) to current moving through the tip. The positive pressure in the pipette was then released and negative suction by hand with a glass syringe applied until the seal resistance reached $\geq 100 \text{ M}\Omega$, at this point a gigaohm seal sometimes formed spontaneously; if the seal was at $\geq 2 \text{ G}\Omega$, experimental cell-attached recording of ion channel activity could start. It was necessary to apply a holding voltage clamp command (-10 to -60 mV) to facilitate gigaohm seal formation. If a gigaohm seal was not formed within 10 min under these conditions the pipette was withdrawn and removed. Formation of a gigaohm seal was again attempted by starting over with a fresh patch pipette.

2.2.6 In-situ Patch Clamp Recording

Upon achieving a gigaohm seal, the patch and unitary currents ~ 10 pA representing BK_{Ca} channel opening were looked for in cell-attached mode. Even if no BK_{Ca} channel activity was observed for recording time of 5 min, the patch pipette voltage was commanded by pClamp to be held for at least 2 min at varying holding potentials from +40 to -80 or 100 mV. Since BK_{Ca} channels are highly voltage sensitive whose P_o increases with patch depolarisation this protocol tested the voltage sensitivity of any currents being recorded, and may have activated BK_{Ca} channels present under the patch that remained in a “deep” close state when $V_{pip} = 0$ mV. In addition, positive or negative pressure was occasionally applied into the patch pipette by hand of about ± 5 -10 hPa since this procedure sometimes activates dormant BK_{Ca} channels in IPANs (Kunze et al., 2000).

Irrespective of whether BK_{Ca} channel opening was recorded during the above protocol, the patch pipette was returned to 0 mV holding potential for ~ 5 min and presynaptic 20 Hz stimulus train was applied to an internodal strand lying just circumferential to the ganglion containing the patched neuron (Mao et al., 2006). This stimulus method reliably evokes sEPSPs in IPANs recorded in current clamp mode; responses are recorded as sEPSPs when the amplifier is in voltage clamp mode, as was the case for our cell-attached recordings. A ~ 5 min post stimulation time-frame was also recorded, post hoc (off line) analysis performed after the experiment detected any changes in BK_{Ca} channel opening that may have been induced by the 20 Hz simulation.

2.2.7 Whole-cell recording

After cell-attached recordings were finished, the whole-cell configuration was attempted. The pClamp software was put into membrane test mode and a voltage command to the pipette was set at -60 mV to prevent a 0 mV command being applied to the cell in whole-cell configuration.

Rupture of the membrane in the pipette was attempted by providing negative pressure. On successfully achieving the small capacitive transients seen in cell-attached mode, transients were increased to reflect the capacitance of the whole soma membrane. Membrane capacitance was again compensated for using the amplifier and series resistance was compensated by ~60%.

The amplifier was next switched to $I = 0$ neutral mode and then to current clamp mode to reduce transient current pulses that are produced when the amplifier switches directly from voltage to current clamp modes. In current clamp mode membrane voltage could be recorded with or without current pulse stimulation of the soma via the patch pipette.

Identification of the patched cell as being of the AH cell phenotype was performed measuring the RMP and responses to a set of current injection protocols (Kunze et al., 2009; Mao et al., 2006). Intrinsic soma excitability was measured by injecting small 500 ms duration depolarising current pulses of increasing intensity until threshold which is the lowest current intensity that evoked a single action potential 50% of the time. Then, action potential accommodation was assessed by injecting a current pulse at twice threshold intensity. The input resistance, and presence of a AH cell defining hyperpolarising cationic current was tested for by injecting 500 ms duration hyperpolarising current pulses until the pulses increased membrane polarisation during injection to -100 mV. The action potential shape and presence and magnitude of the sAHP were determined by evoking 1 or 3 action potentials by injecting a narrow (~5 ms duration) depolarising current pulse of increasing intensity until the action potential was evoked after the electrotonic voltage response to the current pulse had returned to baseline or near the baseline. This allowed uncontaminated measurement of action potential amplitude and half width (width of the spike at half its amplitude from RMP). In AH cells (IPANs) the action potential spike is followed by a sAHP with parameters can also be measured in later analysis.

2.2.8 Morphological Identification of Myenteric Neurons

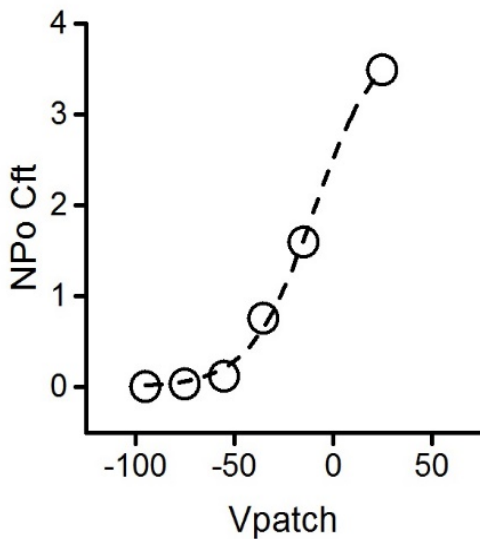
The microelectrode used to record cell-attached and whole cell voltage and current respectively was filled with 1 % Neurobiotin tracer prior to experiment onset. At the end of the experiment, the following protocol was used to inject the Neurobiotin tracer into the AH cell: injection of 500 ms current with threshold intensity (as previously determined), repeating this injection once every second for 10 minutes. Cells were allowed to sit in the carboxygenated Krebs for at least 30 minutes following the injection protocol to allow the tracer to migrate from the soma down the axons and processes. Preparations were then removed from the recording microscope and fixed with 4% paraformaldehyde fixative overnight where it was covered and placed at 4°C. The preparation was then washed with PBS-TX (PBS-triton X; 0.05 M with 0.3% TX-100, pH 7.4) 3 times for ten minutes each time. Next, the preparation was stained in a solution containing 10 µL avidin-Texas Red: 2 mL PBS-TX and incubated for 90 minutes at room temperature in the dark. The tissue preparation was then washed 3 times for ten minutes each time using the PBS-TX. After this, the tissue was mounted on a microscope slide and covered with a covered slide and put into the fridge over night at 4°C. Tissues were then imaged using an inverted Zeiss axio observer microscope (Zeiss, <https://www.zeiss.com>).

2.2.9 Statistical analysis

Values are expressed as mean \pm S.E.M. Statistical analyses were conducted using GraphPad Prism 6. For comparisons between the means of control and experimental conditions on the same cells, a paired t-test was used with $\alpha = 0.05$.

2.3 Results

BK_{Ca} channels responded differentially to voltage commands. Their open probability increased with depolarisation of the IPAN membrane within the patch clamp electrode. Open probability was measured as NP_o which is a product of the number (N) of active BK_{Ca} channels within the patch multiplied by the open probability (P_o). NP_o was plotted against the transpatch potential (V_{intracellular} – V_{extracellular}) and then fitted with the Boltzmann equation (Figure 4) (Kunze et al., 2000). The slope (dx) of the Boltzmann curve at half maximum, and the voltage at which the Boltzmann is half maximum (x₀) were measured for each IPAN that was successfully patched and which had stationary BK_{Ca} channels. For 10 neurons dx was 16.3 ± 2.4 and x₀ = 17.3 ± 4.2 mV.



Model	Boltzmann
Equation	$y = A2 + (A1-A2)/(1 + \exp((x-x0)/dx))$
Plot	NPo Cft
A1	0 ± 0
A2	3.88357 ± 0.20417
x0	-9.78249 ± 2.93863
dx	15.95724 ± 1.88257
Reduced Chi-Sqr	0.00645
R-Square(COD)	0.99793
Adj. R-Square	0.99655

Figure 4. Representative illustration of one IPAN for the NP_o (the open probability (P_o) x number of channels within the patch (N)). BK_{Ca} channels varies with trans-patch potential. Depolarisation increased NP_o; data points were fitted with the Boltzmann equation.

Plot of unitary conductance versus trans-patch voltage for a representative BK_{Ca} channel. The slope of the line fitted to the plot gave unitary conductance of 189 pS. The unitary conductance of single BK_{Ca} channels follows Ohm's law and was determined by plotting unitary current against trans-patch voltage. The slope of the line fitted through the current voltage plot gives the unitary conductance for the channel. For 10 BK_{Ca} channels recorded from 10 IPANs the unitary conductance was 191 ± 22 pS (Figure 5).

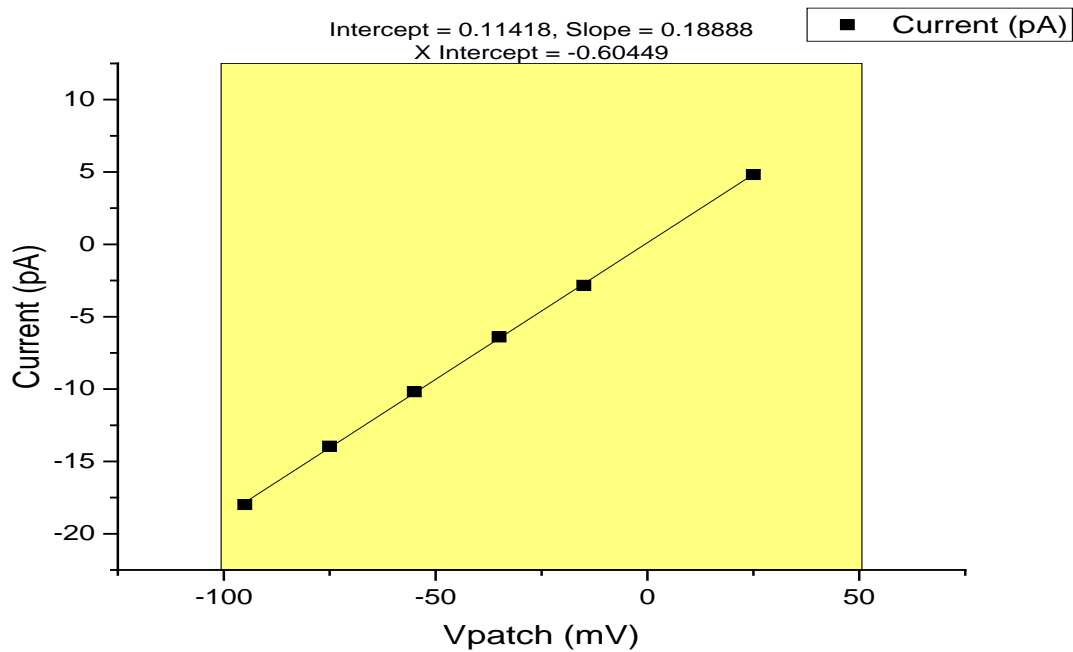
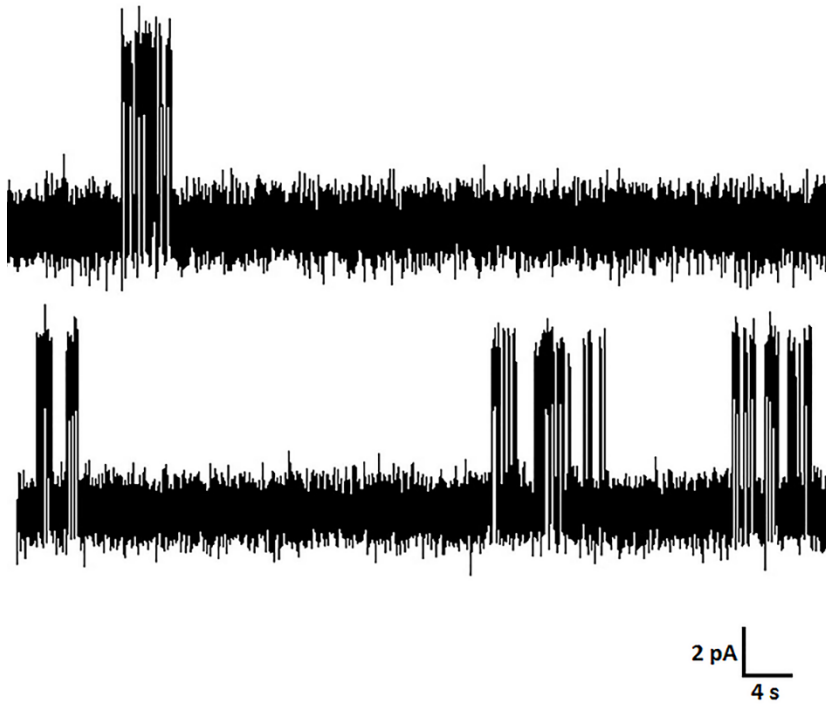


Figure 5. Representative illustration of one I-V plot for BK_{Ca} channel unitary conductance.

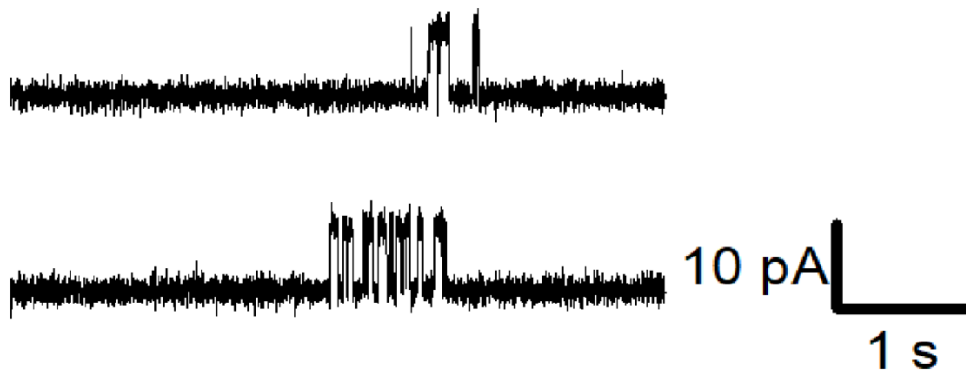
Slow EPSPs were evoked in IPANs by stimulating presynaptic axons (neurites) running in internodal strands between adjacent myenteric ganglia. The stimulus parameters were 10 cathodal current pulses with 0.5 ms duration, delivered at 20 Hz frequency. These parameters reliably evoke slow EPSPs in the target neuron (Kunze et al., 2000). Presynaptic stimulation was followed by an increase in BK_{Ca} channel opening within 10-20 s of the onset to the stimulus pulse train. Figure 6 shows the effect of a sEPSP on BK_{Ca} channel(s) in a single patch; after presynaptic stimulation channel opens more frequently. Figure 7 shows summary data taken from 10 BK_{Ca} channels recorded from 10 mice. NP_o increased by 111% from 0.035 ± 0.014 to 0.074 ± 0.021 ($P = 0.0096$).

A1



B1

A2



B2

Figure 6. Representative cell-attached patch clamp current recording of the effect of presynaptic stimulation at 20 Hz.

Presynaptic stimulation increased BK_{Ca} channel NP_o. For 2 IPANs the stimulation had no apparent effect, possibly because the patch did not contain BK_{Ca} channels or the presynaptic stimulus electrode did not excite axons projecting onto the neuron being recorded from.

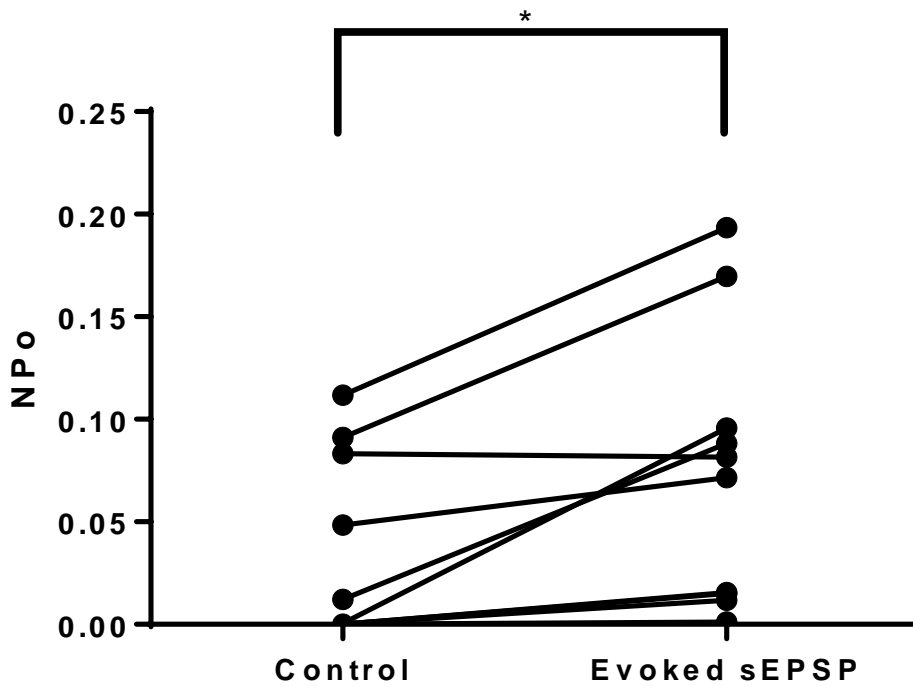


Figure 7. Effect of slow EPSP on BK_{Ca} channel NP_o. Summary graph of BK_{Ca} channel activity prior and post evocation of sEPSPs.

Digital image of Neurobiotin-filled, multi-axonal neuron for which sEPSP stimulation increased BK_{Ca} channel activity. 6/10 IPANs were successfully filled with 1% Neurobiotin marker and successfully recovered after histological treatment. All had multiple long processes arising from the soma (see Figure 8 where the arrow points to the soma), confirming the Dogiel type II morphotype.

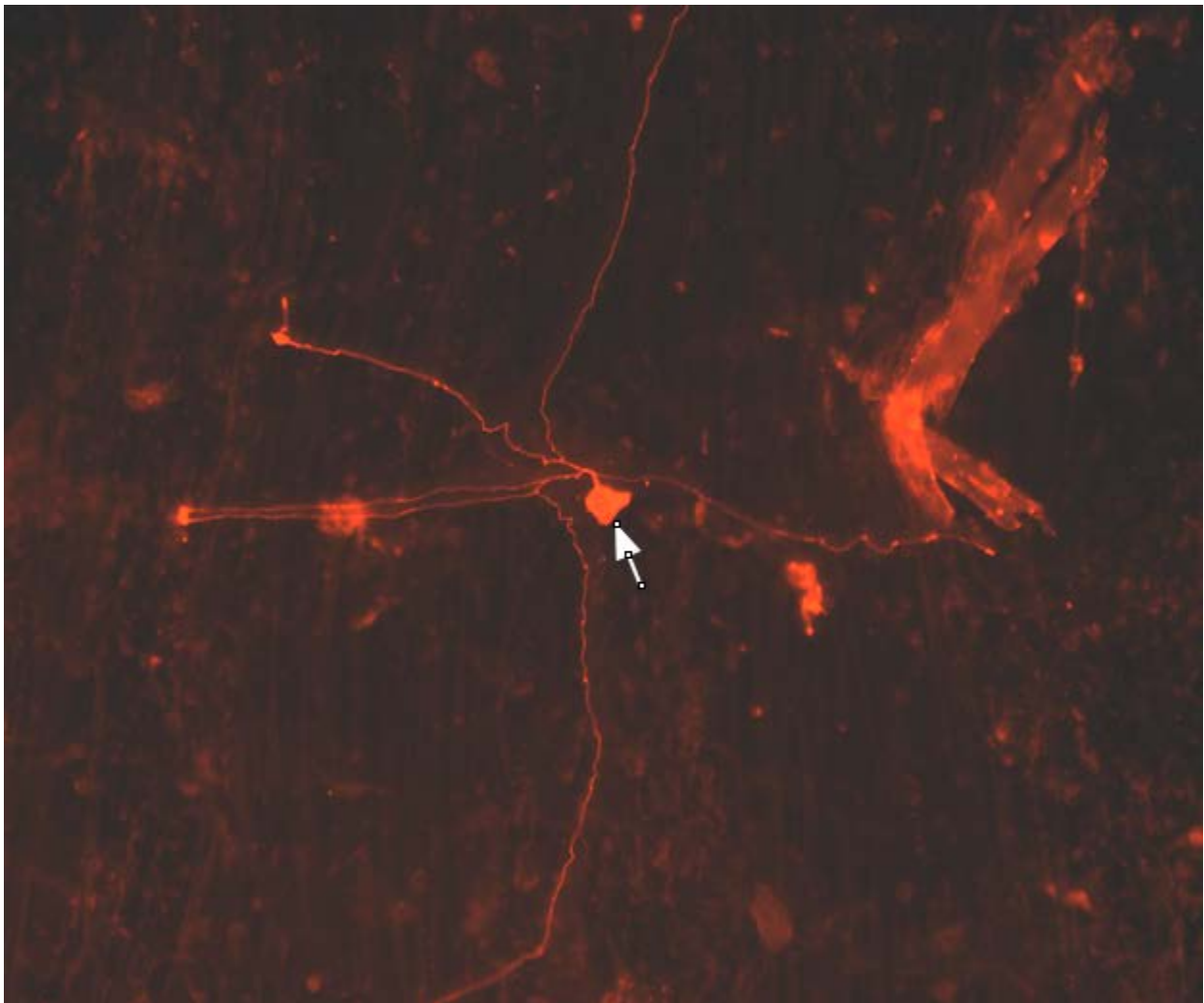


Figure 8. Dogiel type II/AH neuron shape.

2.4 Discussion

Electrophysiological characteristics of BK_{Ca} channels

We characterised K⁺ channels with large unitary currents electrophysiologically to identify BK_{Ca} channels. Our K⁺-rich patch clamp pipette solution ensured that these channels passed K⁺ rather than Cl⁻ ions because the [Cl⁻] was kept low by substituting KMeSO₄ for the anion (Methods). Although, there is a sizeable number of K⁺ channels in IPANs, all have a smaller conductance and therefore smaller unitary currents than BK_{Ca} channels. All the channels that were tested for responses to presynaptic slow EPSP stimulation had a unitary conductance of about 200 pS and were voltage sensitive (Results). These channels were also steeply voltage dependent, meaning that their open probability (NP_o) increased with increasing trans-patch depolarisation. We have previously found that K⁺ channels with these attributes in IPANs were also Ca²⁺-dependent; that is, their open probability increases with increasing concentrations of intracellular Ca²⁺ (Kunze et al., 2000). We therefore identified a large conductance K⁺ channels as BK_{Ca} channels, although we acknowledge that additional confirmation of their Ca²⁺ sensitivity is desirable in the future.

Slow excitatory post-synaptic potential effects on myenteric BK_{Ca} channels

Slow (metabotropic) synaptic IPAN to IPAN neurotransmission is important for normal motility of the intestine (Kunze et al., 2000). Although IPANs transmit to other IPANs and motor- or interneurons, the latter two do not normally transmit back to IPANs (Kunze et al., 1993). The neurotransmitters involved in this metabotropic synaptic transmission have not been fully elucidated. In the guinea pig they include substance P, but in the mouse, they have not yet been identified. However, murine IPANs are strongly immunoreactive for calcitonin gene-related peptide (CGRP) (Furness et al., 2004), a transmitter acting on excitatory metabotropic receptors.

Nevertheless, presynaptic stimulation of internodal strand fibres with a short 20 Hz train after total pulses evokes robust slow excitatory postsynaptic potentials and currents in myenteric mouse IPANs (Mao et al., 2006).

There are 2 types of Ca^{2+} dependent K^+ that influence IPAN excitability. The intermediate conductance Ca^{2+} dependent K^+ channel (IK_{Ca}), is voltage independent and has a unitary conductance of 20-70 pS. It is thus easily differentiated electrophysiologically from the BK_{Ca} channel. The IK_{Ca} is responsible for the generation of the slow afterhyperpolarisation (sAHP) that follows the IPAN action potential upstroke after a delay of several hundred ms. The BK_{Ca} contributes to the fast afterhyperpolarisation (fAHP) which immediately follows the upstroke of the action potential. The fAHP is also referred to in the literature as the “undershoot” or the action potential “anti-peak”; we use these terms.

During the sEPSP the intrinsic excitability of IPAN is increased, largely by the inhibition of the sAHP due to a decrease in IK_{Ca} open probability (Mao et al., 2006). We hypothesised in the Introduction that BK_{Ca} open probability is similarly decreased by the sEPSP. However, our results falsify this hypothesis as they clearly show, for the first time, that BK_{Ca} channels increase their open probability during the sEPSP.

CHAPTER 3: OPENING AND BLOCKING BK_{Ca} CHANNELS PHARMACOLOGICALLY TO DETERMINE THE EFFECTS BK_{Ca} CURRENT HAS ON WHOLE-CELL IPAN ELECTROPHYSIOLOGICAL PARAMETERS

3.1 Introduction

Findings from the initial experiments suggested that sEPSPs increased the NP_o of BK_{Ca} channels expressed on IPANs. This chapter explores what this increased activity of the BK_{Ca} channel mean for the intrinsic properties of IPANs. An Agonist (NS-19504) was chosen due to its selectivity and specificity of BK_{Ca} channels along with its preferable lower optimal working range compared to other agonists. The purpose of the opener was to mimic increased activity found in the first experiments to emphasize the potential effects on IPAN characteristics such as rheobase (threshold), and twice the minimum threshold peak and anti-peak of action potentials etc. A well-known and used blocker of BK_{Ca} channels (paxilline) was chosen as well to block the potential intrinsic effects of BK_{Ca} channels on the excitability of IPANs. These experiments were run alongside controls on the same IPANs prior to application of drugs. The importance of these experiments is to understand the mode of action by which BK_{Ca} channels effect IPANs' properties and what specific properties if any rely on BK_{Ca} channels.

3.2 Methods

3.2.1 Animals

Adult male Swiss Webster (SW) mice (20–30 g, ~3–4 months old) were procured from Charles River Laboratories (Wilmington, MA, USA). After >1-week acclimatization in the St Joseph's animal facility, mice were transported to the laboratory and killed by cervical dislocation. All ensuing procedures were ex-vivo. All animal protocols were covered by the McMaster animal utilisation protocol #160830.

3.2.2 Tissue preparation

After the mouse was sacrificed, it was placed ventral side up on a cork board and spread out using 22-gauge syringe needles to impale fore and hind paws. The skin was opened by a vertical midline abdominal incision and retracted to expose the underlying muscle. The abdominal skeletal muscle coat was opened with another vertical midline incision using surgical scissors and retracted to expose the viscera. A 3-4 cm segment of middle jejunum was excised, taking care not to unduly stretch the attached mesentery and vessels nor to touch or stretch the segment. The segment was freed from the adherent mesentery by cutting with surgical scissors and placed in a recording chamber made using a polystyrene petri dish (Falcon 1006, 50 mm×9 mm, Becton Dickinson, NJ, USA). The bottom of the dish was lined 2 mm deep with cured silicone elastomer (Sylgard®, Dow Corning, MI, USA) and filled with cold Krebs saline (composition in mM: NaCl 118.1, KCl 4.8, NaHCO₃ 25, NaH₂PO₄ 1.0, MgSO₄ 1.2, glucose 11.1, and CaCl₂ 2.5) to which 3 μM nifedipine (Sigma-Aldrich, Oakville, CA) and 10 μM scopolamine (Sigma-Aldrich, Oakville, CA) had been added. The saline was oxygenated and pH buffered by being continuously gassed with carbogen (95% O₂, 5% CO₂).

The following dissection was carried out using a Nikon eclipse inverted microscope (Nikon Instruments Inc, <https://www.nikoninstruments.com>) with 40 × magnification. The mesenteric attachment was dissected away using fine surgical scissors and the jejunal segment opened by cutting in the oral to anal direction along the line of mesenteric attachment. The open segment was pinned flat with mucosa uppermost using 2 cm long insect pins at each corner with the oral edge uppermost in the dish. Using fine dissection forceps and starting at the anal end the mucosa and submucosa were gently lifted off the underlying circular muscle and progressively teased away until it was entirely removed. Now, the tissue was re-pinned and stretched using 40 μm diameter

tungsten wire pins to anchor the edges. The circular muscle was then carefully removed by microdissection taking care to minimise damage to the underlying myenteric plexus. When 50% or more of the circular muscle had been removed the tissue in the recording chamber was allowed to rest by being placed in a glass beaker filled with 1 L oxygenated Krebs saline with nicardipine and scopolamine.

3.2.3 Electrophysiology Setup

The tissue and recording chamber were placed onto the stage of a Nikon eclipse inverted microscope (Nikon Instruments Inc, <https://www.nikoninstruments.com>) and the tissue perfused (4 mL/min) with prewarmed (35°C) oxygenated Krebs saline and nicardipine/scopolamine driven by a VWR heated peristaltic pump (VWR, <https://us.vwr.com>). An earth return consisting of a chlorided 2 cm long silver wire was placed into the Krebs saline in the recording chamber. The return was connected to the common earth input of the recording amplifier. Enzymes or drugs were delivered onto the tissue via a 200-300 µm diameter glass pipette by gravity feed from a 10 mL plastic syringe positioned 20 cm above recording chamber.

The microscope was mounted on a TMC vibration isolation table (Technical Manufacturing Corporation, <http://www.techmfg.com>) and the whole surrounded by a grounded Faraday cage to isolate them from electric fields (see figure 2). The recording electrode consisted of a chloride silver wire inserted into a patch pipette holder which was connected to an Axon Instruments MultiClamp 700B computer amplifier (Molecular Devices, Sunnyvale, CA, USA) which could record voltage signals in current clamp mode or currents in voltage clamp mode. The amplified signals were fed into an Axon Instruments Digidata 1550B digitiser (Molecular Devices, Sunnyvale, CA, USA) which converted the analog signals to digital ones which could be displayed

in real-time on a PC computer running pClamp 10 (Axon Instruments) software and was stored on computer disc for post-hoc analysis.

3.2.4 Sharp Electrode Preparation

Patch pipettes were manufactured from thick-walled borosilicate glass tubing (ID = 0.86 mm, OD = 1.5 mm, BF150-86-10, Sutter instruments) using a Brown-Flaming P-97 programmable pipette puller (Sutter instruments). The sharp electrode solution used to fill the pipette was a 1 M KCl solution with 1% Neurobiotin tracer (Vector Laboratories, <https://vectorlabs.com>), and 14 mM KOH added to bring the pH to 7.3). The parameters of the pipette puller were adjusted so that the electrodes had a resistance of 100 to 150 M Ω when the tip was placed within Krebs saline. Each pipette was filled just before use and inserted into the patch pipette holder of the amplifier head stage.

3.2.5 Sharp Electrode Recording

The pClamp software was put into gap-free protocol in the current clamp mode whole cell protocol and a voltage command to the pipette was set at -60 mV to prevent a 0 mV command being applied to the cell in whole-cell configuration. The resistance for bridge balance was then adjusted until the tip resistance was found to be within an appropriate range 100 – 150 M Ω . Once the sharp electrode's tip resistance was within range, the electrode was lowered with the micromanipulator until the tip was touching the somata, which was identified by a drop-in voltage. Once touching the surface, a 50 μ s zap was giving to break into the somata. If successful, a reading of ~60 mV would signify being in the cytoplasm.

Identification of the patched cell as being of the AH cell phenotype was performed measuring the RMP and responses to a set of current injection protocols (Kunze et al., 2009; Mao et al., 2006). Intrinsic soma excitability was measured by injecting small 500 ms duration

depolarising current pulses of increasing intensity until threshold which is the lowest current intensity that evoked a single action potential 50% of the time. Then, action potential accommodation was assessed by injecting a current pulse at twice threshold intensity. The input resistance, and presence of a AH cell defining hyperpolarising cationic current was tested for by injecting 500 ms duration hyperpolarising current pulses until the pulses increased membrane polarisation during injection to -100 mV. The action potential shape and presence and magnitude of the sAHP were determined by evoking 3 action potentials by injecting a narrow (~5 ms duration) depolarising current pulse of increasing intensity until the action potential was evoked after the electrotonic voltage response to the current pulse had returned to baseline. This allowed uncontaminated measurement of action potential amplitude and half width (width of the spike at half its amplitude from RMP). Once the initial identification of the AH cell had been completed, protocols were repeated on the same cells with a 5 μ M paxilline solution (BK_{Ca} channel blocker) was perfused (4 mL/min) at (35°C) for 5 minutes. The same procedure was followed for both the control and with a 10 μ M NS-19504 (BK_{Ca} channel opener).

3.2.6 Morphological Identification of Myenteric Neurons

The microelectrode used to record cell-attached and whole cell voltage and current respectively was filled with 1 % Neurobiotin tracer prior to experiment onset. At the end of the experiment, the following protocol was used to inject the Neurobiotin tracer into the AH cell: injection of 500 ms current with threshold intensity (as previously determined), repeating this injection once every second for 10 minutes. Cells were allowed to sit in the carboxygenated Krebs for at least 30 minutes following the injection protocol to allow the tracer to migrate from the soma down the axons and processes. Preparations were then removed from the recording microscope and fixed with 4% paraformaldehyde fixative overnight where it was covered and placed at 4°C.

The preparation was then washed with PBS-TX (PBS-triton X; 0.05 M with 0.3% TX-100, pH 7.4) 3 times for ten minutes each time. Next, the preparation was stained in a solution containing 10 μ L avidin-Texas Red: 2 mL PBS-TX and incubated for 90 minutes at room temperature in the dark. The tissue preparation was then washed 3 times for ten minutes each time using the PBS-TX. After this, the tissue was mounted on a microscope slide and covered with a covered slide and put into the fridge over night at 4°C. Tissues were then imaged using an inverted Zeiss axio observer microscope (Zeiss, <https://www.zeiss.com>).

3.2.7 Statistical analysis

Values are expressed as mean \pm S.E.M. Statistical analyses were conducted using GraphPad Prism 6. For comparisons between the means of control and experimental conditions on the same cells, a paired t-test was used with $\alpha = 0.05$. The sample size is 6 for all figures, unless removed with Grubb's test to identify outliers.

3.3 Results

Effects of BK_{Ca} channel opener (NS-19504) or blocker (paxilline) on IPAN electrophysiological parameters

To determine if modulation of BK_{Ca} channels affects the minimum firing threshold we first measured the rheobase. The 500 ms duration threshold current passed through a sharp intracellular microelectrode was required to evoke a single action potential in impaled IPANs. This was measured before and after adding the drugs to the Krebs solution perfusing the LMMP preparation. The BK_{Ca} channel opener increased sample rheobase by 36% from 98.0 ± 24.4 to 134.0 ± 22.9 pA (N = 6, p = .34). The blocker decreased rheobase by 53% from 185.0 ± 50.3 to 86.7 ± 14.3 pA (N = 6, p = .13) (Figure 9).

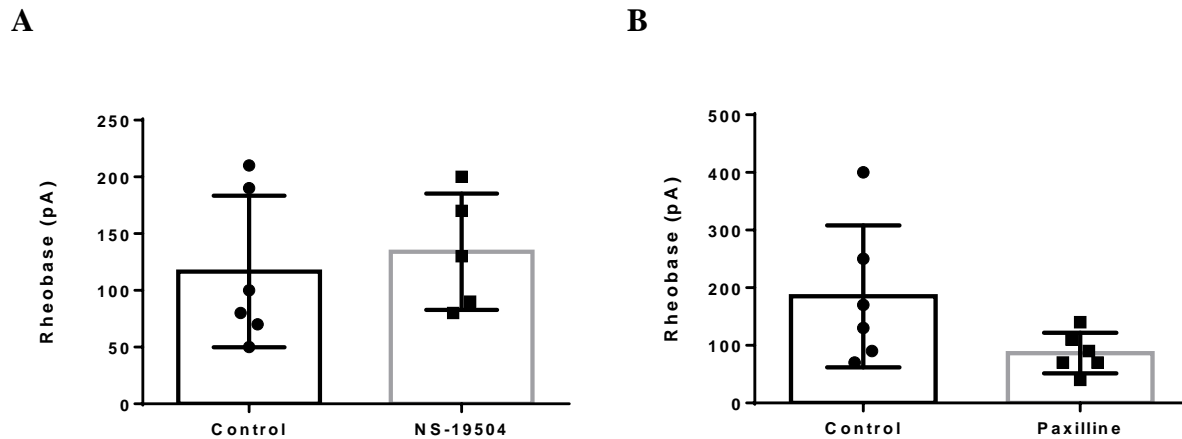


Figure 9. Effects of BK_{Ca} open probability modulators on rheobase. Summary bar graphs of effects of BK_{Ca} channel opener (NS-19504) or blocker (paxilline) on action potential threshold (rheobase). In this and all subsequent summary graphs bars indicate means, errors are standard error or the mean and dots give individual values, N = 6 per each figure.

Intrinsic excitability was measured as the number of action potentials evoked by 500 ms duration intracellular current stimulation at 2x rheobase intensity. No apparent change in sample effect on the number of action potentials was observed before 3.2 ± 0.4 action potentials and after treatment with NS-19504, 3.2 ± 0.7 action potentials ($N = 6$, $p = .99$). Paxilline increased the sample number of action potentials by 28% from 4.3 ± 1.0 to 5.5 ± 0.8 ($N = 6$, $p = .43$) (Figure 10).

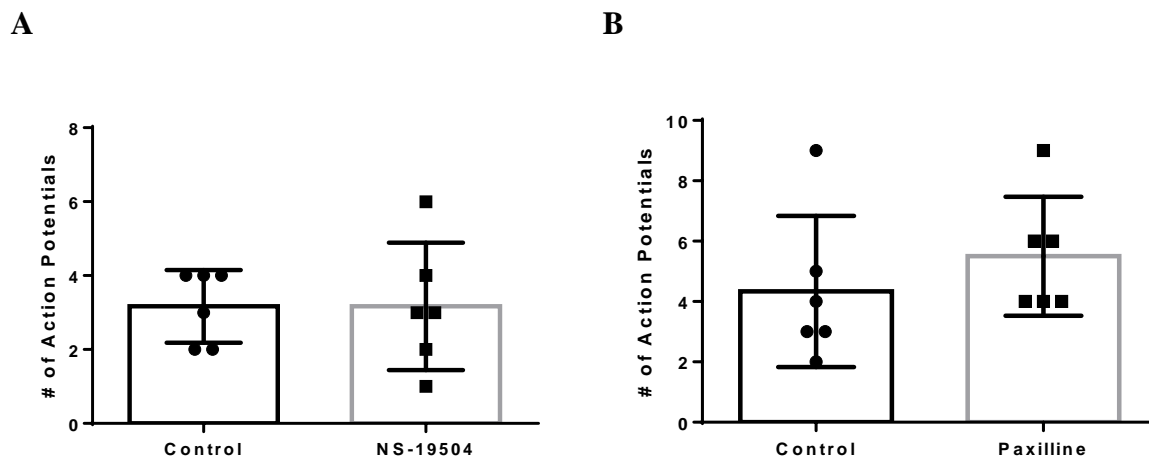


Figure 10. Effects of BK_{Ca} channel open probability modulators on IPAN intrinsic excitability. Summary graphs showing the results of the BK_{Ca} channel opener (NS-19504) (A) and blocker (paxilline) (B) on the number of action potentials evoked by intracellular stimulation at 2 times rheobase intensity. $N = 6$ per each figure.

The effects of BK_{Ca} opener or blocker on the resting membrane potential (RMP) was measured to test for the effects of background (constitutive) openings of BK_{Ca} channels. A) The BK_{Ca} channel opener increased sample membrane polarisation by 4% from -56.8 ± 1.7 mV before adding NS-19504 to -58.7 ± 2.0 mV (N = 6, p = .34). B) The blocker decreased sample polarisation by 5% from -62.3 ± 3.1 to -59.3 ± 4.1 mV (N = 6, p = .13) (Figure 11).

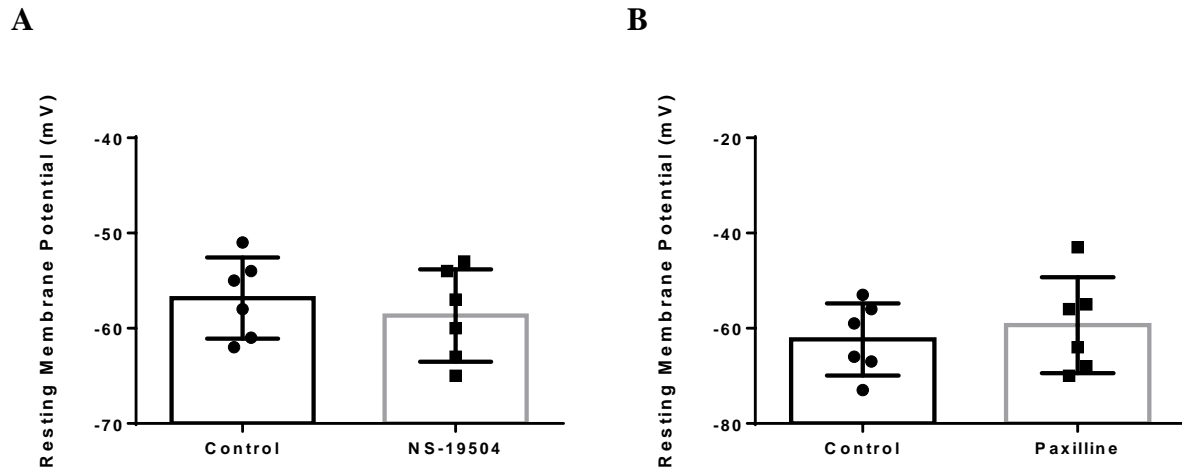


Figure 11. Effects of BK_{Ca} opener or blocker on IPAN resting membrane potential. Summary graphs showing the effects of BK_{Ca} opener or blocker on membrane polarisation (resting membrane potential). N = 6 per each figure.

The amplitude of the fAHP or undershoot was measured after the repolarisation phase of action potentials. The BK_{Ca} channel opener appeared to decrease the absolute sample magnitude of the fAHP amplitude by 44% from -0.9 ± 0.3 mV to -0.5 ± 0.3 mV ($N = 6$, $p = .51$) in the presence of the opener. Paxilline increased the sample fAHP amplitude by 166% from -0.3 ± 0.1 to -0.8 ± 0.1 mV ($N = 6$, $p = .0034$) (Figure 12).

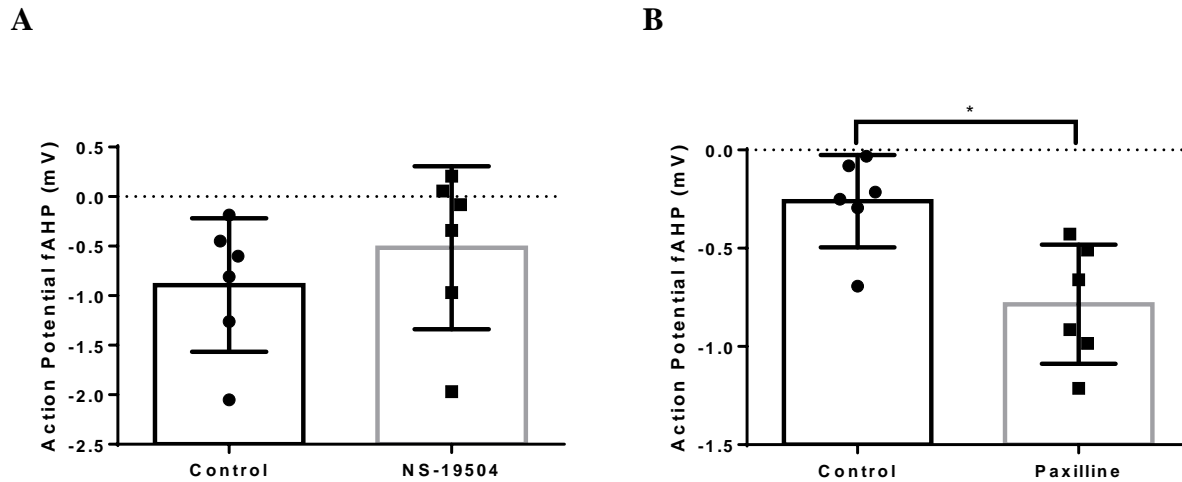


Figure 12. Effects of BK_{Ca} channel opener or blocker on action potential fast afterhyperpolarisation (undershoot). Summary graphs showing the effects of BK_{Ca} opener or blocker on the fast afterhyperpolarization (undershoot). (A) represents the opener, while (B) represents the blocker. $N = 6$ per each figure.

Maximum decay rates were measured during the repolarisation phase of action potentials. The BK_{Ca} channel opener increased the decay rate by 114% from -3.5 ± 0.6 to -7.5 ± 1.2 mV/ms (N = 5, p = .042). The blocker decreased the decay rate by 40% from -5.7 ± 0.8 to -3.4 ± 0.5 mV/ms (N = 6, p = .024) (Figure 13).

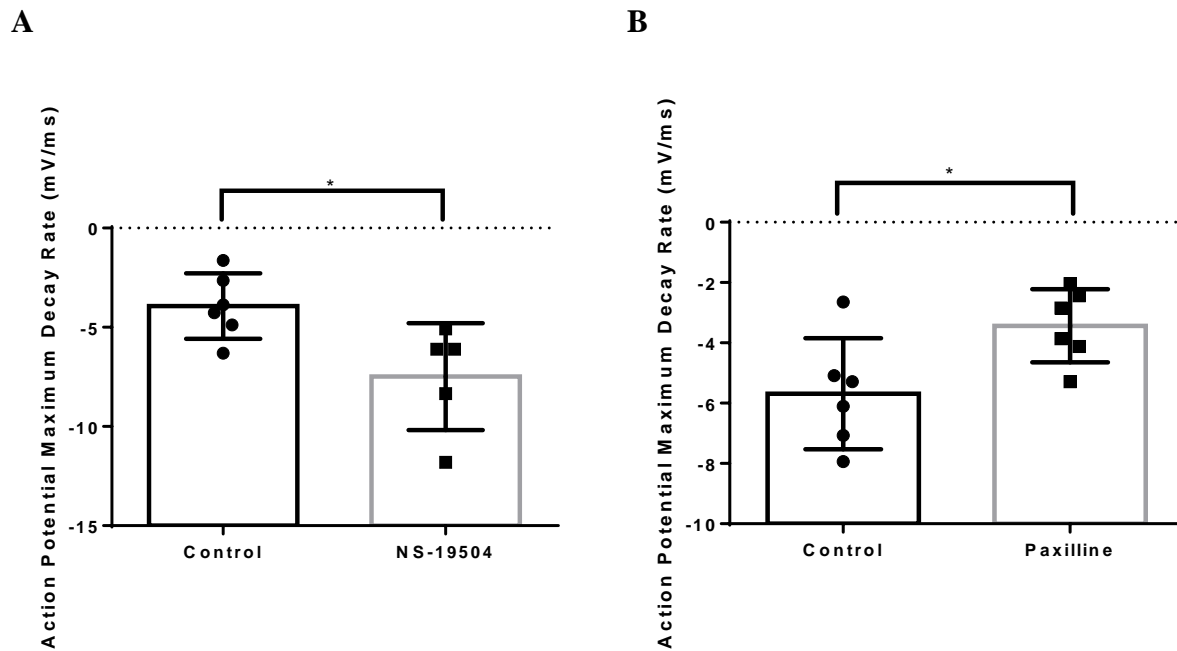


Figure 13. Effects of BK_{Ca} modulators on action potential maximum decay rate. Summary graphs showing the effects of BK_{Ca} opener or blocker on the action potential decay rate. (A) represents before and after the opener was perfused onto the myenteric plexus. (B) represents before and after the blocker was perfused onto the myenteric plexus. N = 6 per each figure.

Modulation of BK_{Ca} channels had varying effects on whole-cell parameters of IPANs. These parameters were measured and analyzed due to their functional association with BK_{Ca} channels throughout physiology. BK_{Ca} channels are believed to have a role in helping to maintain the RMP and determining excitability, these parameters help to measure and describe these functions. The significant effects were on the fast afterhyperpolarization amplitude, and the decay rate of repolarisation. Table 1 lists various parameter values, effects, and trends observed which are summarized below.

Table 1. Effects of BK_{Ca} channel modulators on whole-cell parameters

	Control	NS-19504	% change	Control	Paxilline	% change
Rheobase	98.0 ± 24.4	134.0 ± 22.9	36**	185.0 ± 50.3	86.7 ± 14.3	-53**
No. of action potentials	3.2 ± 0.4	3.2 ± 0.7	0	4.3 ± 1.0	5.5 ± 0.8	28
Resting membrane potential (mV)	-56.8 ± 1.7	-58.7 ± 2.0	4	-62.3 ± 3.1	-59.3 ± 4.1	-5
fAHP amplitude (mV)	-0.9 ± 0.3	-0.5 ± 0.3	-44**	-0.3 ± 0.1	-0.8 ± 0.1	166*
Action potential decay rate (mV/ms)	-3.5 ± 0.6	-7.5 ± 1.2	114*	-5.7 ± 0.8	-3.4 ± 0.5	-40*

* designated as significant $p \leq .05$; ** designated as trends $p \leq .1$

3.4 Discussion

Effects of modulating BK_{Ca} channels on IPAN firing

In the previous chapter we have shown that the sEPSP increases BK_{Ca} open probability (NP_o). To explore what that might mean in terms of the electrophysiological properties of individual IPANs we used BK_{Ca} channel modulators (opener or blocker that increase or decrease NP_o respectively). We measured 5 parameters before and after adding NS-19504 (opener) or paxilline (blocker); namely, rheobase, the number of action potentials discharged at twice rheobase intensity, membrane polarisation (RMP), amplitude of the fAHP and action potential decay rate. We did not measure the magnitude of the sAHP as this is generated by opening of IK_{Ca} rather than BK_{Ca} ion channels.

The results for this section mostly show trends, that is, effect sizes that are not accompanied by statistical significance ($P \leq 0.05$). Nevertheless, we will try to interpret what these trends mean, while acknowledging that larger sample sizes are required.

The BK_{Ca} channel opener (NS-19504) increased rheobase (action potential threshold) by 36%, had no apparent effect on the number of action potentials fired, hyperpolarised the membrane potential by 4%, decreased fAHP amplitude by 44% and increased the action potential decay rate by 114%. The increase in rheobase is consistent with increased BK_{Ca} NP_o increasing the background (leak) current requiring a larger intracellular injection of depolarising current to move the membrane potential to threshold, also this increase in [K⁺] would cause the electrochemical gradient to shift, and require correcting via the Na⁺-K⁺ pump and other electrogenic pumps. The increased membrane polarisation would also move the RMP further away from threshold. The fAHP amplitude was decreased although the BK_{Ca} channel is normally thought to contribute to the fAHP. One explanation for this anomaly may be that since the opener hyperpolarised the neuron

membrane potential thus moving it closer to the K^+ reversal potential, the driving force (K^+ reversal potential - RMP) for the fAHP was decreased. In future studies, the fAHP should be measured in voltage clamp mode where the membrane potential is kept constant. The increase in action potential decay rate is consistent with the role of BK_{Ca} channels in contributing to action potential repolarisation (Tsantoulas & McMahon, 2014; Zhang, Gopalakrishnan, & Shieh, 2003).

Generally, the effects of paxilline were the opposite of NS-19504. The membrane depolarisation indicates the presence of constitutively open BK_{Ca} channel at RMP whose NP_o is decreased by the blocker. The decreased rheobase can be explained by the decreased leak current due to BK_{Ca} channel closure and the reduced polarisation moving membrane potential closer to threshold. The increased fAHP is anomalous but can be explained by the same factors that apply to the BK_{Ca} channel opener in reverse; namely, the paxilline-induced membrane depolarisation increased the driving force for the K^+ channels involved in generating fAHP. The decreased action potential decay rate is consistent the active role that the voltage-sensitive BK_{Ca} plays in action potential repolarisation (see also above). The increased number of action potentials fired would have resulted from the decreased leak (background) currents due to the blockade of open BK_{Ca} channels. The decreased leak conductance produces an increase in “input resistance” which according to ohms law ($V=IR$) means that a given stimulus current will produce a greater change in voltage. In other words, after BK_{Ca} channel blockade the injected stimulus current will produce a larger depolarising voltage deflection which will elicit a greater number of action potentials (see figure 2 in Kunze et al. 1997).

Overall the experiments with pharmacological manipulation of BK_{Ca} NP_o indicate that an increase in BK_{Ca} channel opening reduces the intrinsic excitability and electroresponsiveness of IPANs. This would serve to reduce excitability during the sEPSP counteracting excitatory effect

of the sAHP inhibition that also occurs during the sEPSP (Mao et al., 2006; Wood & Kirchgessner, 2004). It has previously been shown that IPAN BK_{Ca} channels open during intestinal contraction to reduce IPAN excitability and that this could be a protective mechanism to prevent neural hyperexcitability during contractions. Similarly, the opening of BK_{Ca} channels during the sEPSP might prevent hyperexcitability or at least limit the degree of neuronal excitation during slow synaptic transmission. Interestingly a beneficial neuroactive probiotics *Lactobacillus rhamnosus* JB-1™ can produce a sEPSP like excitation in IPANs when the probiotic is applied to the epithelium (Mao et al., 2013). Future experiments should test whether JB-1 and other neuroactive probiotics modulate BK_{Ca} channel activity in IPANs.

CHAPTER 4: CONCLUSION

4.1 Clinical Implications and Topics of future research

The current research findings particularly the effects of sEPSPs on IPANs and their BK_{Ca} channels and the modulatory effects of BK_{Ca} channels on IPANs provides an opportunity to explore gut-associated pathology. Because IPANs in combination with sEPSP are important for propagating contractile complexes within the gut, the results presented allow for targeted therapeutics for dysmotility.

In this thesis, the data presented here demonstrates that sEPSPs increase BK_{Ca} channel activity, BK_{Ca} channels are required for the shaping of action potentials, determining the anti-peak, and have some role in maintaining the resting membrane potential. With this knowledge, there are two avenues of interest where future research could proceed, the first of which is recording these channels with the application of probiotics such as *L. rhamnosus* JB-1. The mechanism of probiotics effects on neurons is still unclear, but it is suggested that IK_{Ca} channels

are involved in the underlying mechanism (Ishii et al., 1997), however, bacterial effects have not been thoroughly investigated on BK_{Ca} channels even though IPANs are thought to be cellular targets of neuroactive bacteria. With this in mind, and evidence supporting that gut bacteria can influence gut motility, a logical experiment would be to record IPANs. Either with a hemi-dissection where bacteria are placed on the mucosa or directly add bacteria onto IPANs via a pico spritzer and record BK_{Ca} channel activity and the intrinsic properties of the cell.

Second, exploring what effects stress has on myenteric IPANs and BK_{Ca} channels would be a viable avenue to explore. It has been reported that BK_{Ca} channels in the lateral amygdala of anxious mice had a reduction in activity, which led to a pronounced reduction in the fAHP, which caused hyperexcitability in these neurons (Guo et al., 2012). Knowing this, a general hypothesis could be generated such as acute stress increases hyperexcitability of IPANs within the jejunum. To test this hypothesis, we could apply acute stress to mice, and record IPAN and BK_{Ca} channel properties, such as we did in this thesis. This would provide a window into what pathology occurs within the gut specifically within the ENS of the jejunum.

4.2 Conclusion

The work reported here demonstrated effects on the ENS through, modulation of BK_{Ca} channels and ultimately IPANs. The connections made between the sEPSP and the BK_{Ca} channel provides an insightful addition to the literature and provides a deeper understanding of how the gut functions on a day to day basis. We demonstrated here that BK_{Ca} channel activity is increased when interacting with sEPSPs, while IK_{Ca} channel activity decreases. We also demonstrated that modulation of BK_{Ca} channels affects IPANs in regards to the anti-peak and decay rate of action potentials. Although we cannot directly conclude that BK_{Ca} channels are solely responsible for these changes in parameters, we observed more negative values of anti-peak amplitude while

blocking BK_{Ca} channels, increased decay rate of the falling phase while opening, and a decreased decay rate while blocking. While electrophysiology is a low throughput art, it remains a necessary tool in understanding how cells interact with pharmacological agents and endogenous agents.

CHAPTER 5: REFERENCES

- Adelman, J. P., Shen, K. Z., Kavanaugh, M. P., Warren, R. A., Wu, Y. N., Lagrutta, A., ... North, R. A. (1992). Calcium-activated potassium channels expressed from cloned complementary DNAs. *Neuron*, 9(2), 209–16. Retrieved from <http://www.ncbi.nlm.nih.gov/pubmed/1497890>
- Atkinson, N. S., Robertson, G. A., & Ganetzky, B. (1991). A Component of Calcium-Activated Potassium Channels Encoded by the *Drosophila slo* Locus Nigel S. Atkinson; Gail A. Robertson; Barry Ganetzky, 253(5019), 551–555.
- Author, N., Hökfelt, T., Kellerth, J. O., Nilsson, G., & Pernow, B. (1975). Substance P: Localization in the Central Nervous System and in Some Primary Sensory Substance P: Localization in the Central Nervous System and in Some Primary Sensory Neurons. *Source: Science, New Series, 190113111*(4217), 889–890. Retrieved from <http://www.jstor.org/stable/1741781>
- Bartschat, D. K., & Blaustein, M. P. (1985). Calcium-activated potassium channels in isolated presynaptic nerve terminals from rat brain. *The Journal of Physiology*, 361, 441–57. Retrieved from <http://www.ncbi.nlm.nih.gov/pubmed/2580982>
- Bornstein, J. C., Furness, J. B., & Kunze, W. A. A. (1994). Electrophysiological characterization of myenteric neurons: how do classification schemes relate? *Journal of the Autonomic Nervous System*, 48(1), 1–15. [https://doi.org/10.1016/0165-1838\(94\)90155-4](https://doi.org/10.1016/0165-1838(94)90155-4)
- Bossaller, C., Reither, K., Hehlert-Friedrich, C., Auch-Schwelk, W., Graf, K., Gräfe, M., & Fleck, E. (1992). In vivo measurement of endothelium-dependent vasodilation with substance P in man. *Herz*, 17(5), 284–90. Retrieved from <http://www.ncbi.nlm.nih.gov/pubmed/1282120>
- Butler, A., Tsunoda, S., McCobb, D. P., Wei, A., & Salkoff, L. (1993). mSlo, a complex mouse gene encoding "maxi" calcium-activated potassium channels. *Science (New York, N.Y.)*, 261(5118), 221–4. Retrieved from <http://www.ncbi.nlm.nih.gov/pubmed/7687074>
- Che, T., Sun, H., Li, J., Yu, X., Zhu, D., Xue, B., ... Liu, C. (2012). Oxytocin hyperpolarizes cultured duodenum myenteric intrinsic primary afferent neurons by opening BK_{Ca} channels through IP₃ pathway. *Journal of Neurochemistry*, 121(4), 516–525. <https://doi.org/10.1111/j.1471-4159.2012.07702.x>
- Clerc, N. (2002). Controlling the excitability of IPANs: a possible route to therapeutics. *Current Opinion in Pharmacology*, 2(6), 657–664. [https://doi.org/10.1016/S1471-4892\(02\)00222-9](https://doi.org/10.1016/S1471-4892(02)00222-9)
- Clerc, N., & Furness, J. B. (2004). Intrinsic primary afferent neurones of the digestive tract. In *Neurogastroenterology and Motility* (Vol. 16, pp. 24–27). <https://doi.org/10.1111/j.1743-3150.2004.00470.x>
- Contreras, G. F., Castillo, K., Enrique, N., Carrasquel-Ursulaez, W., Castillo, J. P., Milesi, V., ... Latorre, R. (2013). A BK (Slo1) channel journey from molecule to physiology. *Channels*, 7(6), 442–458. <https://doi.org/10.4161/chan.26242>

- Dogiel, A. S. (1899). Über den Bau der Ganglien in den Geflechten des Darmes und der Gallenblase des Menschen und der Säugetiere. *Arch. Anat. Physiol.(Leipzig) Anat. Abt. Jg.*, 1899, 130-158.
- Donkin, J. J., Turner, R. J., Hassan, I., & Vink, R. (2007). Substance P in traumatic brain injury. *Progress in Brain Research*, 161, 97–109. [https://doi.org/10.1016/S0079-6123\(06\)61007-8](https://doi.org/10.1016/S0079-6123(06)61007-8)
- Ekblad, E., Winther, C., Ekman, R., Ha°kanson, R., & Sundler, F. (1987). Projections of peptide-containing neurons in rat small intestine. *Neuroscience*, 20(1), 169–188. [https://doi.org/10.1016/0306-4522\(87\)90010-8](https://doi.org/10.1016/0306-4522(87)90010-8)
- Eyzaguirre, C., & Kuffler, S. W. (1955). Processes of excitation in the dendrites and in the soma of single isolated sensory nerve cells of the lobster and crayfish. *The Journal of General Physiology*, 39(1), 87–119. Retrieved from <http://www.ncbi.nlm.nih.gov/pubmed/13252237>
- Ferens, D. M., Chang, E. C., Bogeski, G., Shafton, A. D., Kitchener, P. D., & Furness, J. B. (2005). Motor patterns and propulsion in the rat intestine in vivo recorded by spatio-temporal maps. *Neurogastroenterology and Motility*, 17(5), 714–720. <https://doi.org/10.1111/j.1365-2982.2005.00684.x>
- Furness, J. B., & Costa, M. (1984). Origins of Peptide and Norepinephrine Nerves in the Mucosa of the Guinea Pig Small Intestine. *Gastroenterology*, 86(4), 637–644. [https://doi.org/10.1016/S0016-5085\(84\)80111-0](https://doi.org/10.1016/S0016-5085(84)80111-0)
- Furness, J. B., Johnson, P. J., Pompolo, S., & Bornstein, J. C. (1995). Evidence that enteric motility reflexes can be initiated through entirely intrinsic mechanisms in the guinea-pig small intestine. *Neurogastroenterology & Motility*, 7(2), 89–96. <https://doi.org/10.1111/j.1365-2982.1995.tb00213.x>
- Furness, J. B., Kunze, W., Bertrand, P., Clerc, N., & Bornstein, J. (1998). Intrinsic primary afferent neurons of the intestine. *Progress in Neurobiology*, 54(1), 1–18. [https://doi.org/10.1016/S0301-0082\(97\)00051-8](https://doi.org/10.1016/S0301-0082(97)00051-8)
- Furness, J. B. (2007). *The Enteric Nervous System*. (J. B. Furness, Ed.), *The Enteric Nervous System*. Malden, Massachusetts, USA: Blackwell Publishing. <https://doi.org/10.1002/9780470988756>
- Furness, J. B., Rivera, L. R., Cho, H.-J., Bravo, D. M., & Callaghan, B. (2013). The gut as a sensory organ. *Nature Reviews Gastroenterology & Hepatology*, 10(12), 729–740. <https://doi.org/10.1038/nrgastro.2013.180>
- Furness, J., Bornstein, J., Kunze, W., Bertrand, P., Kelly, H., & Thomas, E. (1996). Experimental Basis for Realistic Large-Scale Computer Simulation of the Enteric Nervous System. *Clinical and Experimental Pharmacology and Physiology*, 23(9), 786–792. <https://doi.org/10.1111/j.1440-1681.1996.tb01180.x>

- Furness, J., Robbins, H., Xiao, J., Stebbing, M., & Nurgali, K. (2004). Projections and chemistry of Dogiel type II neurons in the mouse colon. *Cell and Tissue Research*, 317(1), 1–12. <https://doi.org/10.1007/s00441-004-0895-5>
- Gershon, M. D. (1999). The Enteric Nervous System: A Second Brain. *Hospital Practice*, 34(7), 31–52. <https://doi.org/10.3810/hp.1999.07.153>
- Guerrant, R. L., Ganguly, U., Casper, A. G., Moore, E. J., Pierce, N. F., & Carpenter, C. C. (1973). Effect of *Escherichia coli* on fluid transport across canine small bowel. Mechanism and time-course with enterotoxin and whole bacterial cells. *The Journal of Clinical Investigation*, 52(7), 1707–14. <https://doi.org/10.1172/JCI107352>
- Guo, Y.-Y., Liu, S.-B., Cui, G.-B., Ma, L., Feng, B., Xing, J.-H., ... Zhao, M.-G. (2012). Acute stress induces down-regulation of large-conductance Ca²⁺-activated potassium channels in the lateral amygdala. *The Journal of Physiology*, 590(Pt 4), 875–886. <https://doi.org/10.1113/jphysiol.2011.223784>
- Gwynne, R. M., & Bornstein, J. C. (2007). Synaptic transmission at functionally identified synapses in the enteric nervous system: roles for both ionotropic and metabotropic receptors. *Current Neuropharmacology*, 5(1), 1–17. <https://doi.org/10.2174/157015907780077141>
- Hendriks, R., Bornstein, J. C., & Furness, J. B. (1990). An electrophysiological study of the projections of putative sensory neurons within the myenteric plexus of the guinea pig ileum. *Neuroscience Letters*, 110(3), 286–290. [https://doi.org/10.1016/0304-3940\(90\)90861-3](https://doi.org/10.1016/0304-3940(90)90861-3)
- Hillsley, K., Kenyon, J. L., & Smith, T. K. (2001). Ryanodine-Sensitive Stores Regulate the Excitability of AH Neurons in the Myenteric Plexus of Guinea-Pig Ileum. *Am J Physiol Cell Physiol*, 280(1), C22–33. Retrieved from <http://ajpcell.physiology.org/cgi/content/abstract/280/1/C22%5Cnpapers://3487cc51-5bdd-41e3-a278-ca18a55f0bd9/Paper/p531>
- Hirst, G. D., Holman, M. E., Prosser, C. L., & Spence, I. (1972). Some properties of the neurones of Auerbach's plexus. *The Journal of Physiology*, 225(2), 60P–61P. Retrieved from <http://www.ncbi.nlm.nih.gov/pubmed/5074417>
- Horrigan, F. T., & Aldrich, R. W. (1999). Allosteric voltage gating of potassium channels II. Mslo channel gating charge movement in the absence of Ca²⁺. *The Journal of General Physiology*, 114(2), 305–36. Retrieved from <http://www.ncbi.nlm.nih.gov/pubmed/10436004>
- Horrigan, F. T., & Aldrich, R. W. (2002). Coupling between voltage sensor activation, Ca²⁺ binding and channel opening in large conductance (BK) potassium channels. *The Journal of General Physiology*, 120(3), 267–305. <https://doi.org/10.1085/jgp.20028605>

- Hunt, S. P., Felipe, C. De, Herrero, J. F., O'Brien, J. A., Palmer, J. A., Doyle, C. A., ... Cervero, F. (1998). Altered nociception, analgesia and aggression in mice lacking the receptor for substance P. *Nature*, *392*(6674), 394–397. <https://doi.org/10.1038/32904>
- Ishii, T. M., Silvia, C., Hirschberg, B., Bond, C. T., Adelman, J. P., & Maylie, J. (1997). A human intermediate conductance calcium-activated potassium channel. *Proceedings of the National Academy of Sciences*, *94*(21), 11651–11656. <https://doi.org/10.1073/pnas.94.21.11651>
- Katsanos, G. S., Anogeianaki, A., Orso, C., Tetè, S., Salini, V., Antinolfi, P. L., & Sabatino, G. (2008). IMPACT OF SUBSTANCE P ON CELLULAR IMMUNITY. *JOURNAL OF BIOLOGICAL REGULATORS & HOMEOSTATIC AGENTS*, 393–974.
- Katz, B. (1950). Depolarization of sensory terminals and the initiation of impulses in the muscle spindle. *The Journal of Physiology*, *111*(3–4), 261–82. Retrieved from <http://www.ncbi.nlm.nih.gov/pubmed/14795439>
- Krnjević, K., & Lisiewicz, A. (1972). Injections of calcium ions into spinal motoneurons. *The Journal of Physiology*, *225*(2), 363–90. Retrieved from <http://www.ncbi.nlm.nih.gov/pubmed/5074394>
- Kunze, W., Bertrand, P. P., Furness, J. B., & Bornstein, J. C. (1997). Influence of the mucosa on the excitability of myenteric neurons. *Neuroscience*, *76*(2), 619–634. [https://doi.org/10.1016/S0306-4522\(96\)00408-3](https://doi.org/10.1016/S0306-4522(96)00408-3)
- Kunze, W., Clerc, N., Furness, J. B., & Gola, M. (2000). The soma and neurites of primary afferent neurons in the guinea-pig intestine respond to differentially deformation. *The Journal of Physiology*, *526*(2), 375–385. <https://doi.org/10.1111/j.1469-7793.2000.00375.x>
- Kunze, W., & Furness, J. B. (1999). THE ENTERIC NERVOUS SYSTEM AND REGULATION OF INTESTINAL MOTILITY. *Annu. Rev. Physiol*, *61*, 117–42.
- Kunze, W., Furness, J. B., Bertrand, P. P., & Bornstein, J. C. (1998). Intracellular recording from myenteric neurons of the guinea-pig ileum that respond to stretch. *Journal of Physiology*, *506*(3), 827–842. <https://doi.org/10.1111/j.1469-7793.1998.827bv.x>
- Kunze, W., Furness, J. B., & Bornstein, J. C. (1993). Simultaneous intracellular recordings from enteric neurons reveal that myenteric ah neurons transmit via slow excitatory postsynaptic potentials. *Neuroscience*, *55*(3), 685–694. [https://doi.org/10.1016/0306-4522\(93\)90434-H](https://doi.org/10.1016/0306-4522(93)90434-H)
- Kunze, W., Mao, Y., Wang, B., Huizinga, J. D., Ma, X., Forsythe, P., & Bienenstock, J. (2009). *Lactobacillus reuteri* enhances excitability of colonic AH neurons by inhibiting calcium-dependent potassium channel opening. *Journal of Cellular and Molecular Medicine*, *13*(8b), 2261–2270. <https://doi.org/10.1111/j.1582-4934.2009.00686.x>
- Laumonier, F., Roger, S., Guérin, P., Molinari, F., Cahard, D., Belhadj, A., ... Briault, S. (1622). Association of a Functional Deficit of the BK Ca Channel, a Synaptic Regulator of Neuronal Excitability, With Autism and Mental Retardation. *Am J Psychiatry*, *163*(9).

- Lauritsen, K., Laursen, L. S., Bukhave, K., & Rask-Madsen, J. (1988). In vivo profiles of eicosanoids in ulcerative colitis, Crohn's colitis, and Clostridium difficile colitis. *Gastroenterology*, *95*(1), 11–17. [https://doi.org/10.1016/0016-5085\(88\)90284-3](https://doi.org/10.1016/0016-5085(88)90284-3)
- Li, Q., & Yan, J. (2016). Modulation of BK Channel Function by Auxiliary Beta and Gamma Subunits. *International Review of Neurobiology*, *128*, 51–90. <https://doi.org/10.1016/bs.irn.2016.03.015>
- Lu, R., Lukowski, R., Sausbier, M., Zhang, D. D., Sisignano, M., Schuh, C.-D., ... Schmidtko, A. (2014). BKCa channels expressed in sensory neurons modulate inflammatory pain in mice. *Pain*, *155*(3), 556–565. <https://doi.org/10.1016/j.pain.2013.12.005>
- Mao, Y., Kasper, D., Wang, B., Forsythe, P., Bienenstock, J., & Kunze, W. (2013). Bacteroides fragilis polysaccharide A is necessary and sufficient for acute activation of intestinal sensory neurons. *Nature Communications* *4*, 1410–1465. <https://doi.org/10.1038/ncomms2478>
- Mao, Y., Wang, B., & Kunze, W. (2006). Characterization of myenteric sensory neurons in the mouse small intestine. *Journal of Neurophysiology*, *96*(3), 998–1010. <https://doi.org/10.1152/jn.00204.2006>
- Mathialahan, T., MacLennan, K., Sandle, L., Verbeke, C., & Sandle, G. (2005). Enhanced large intestinal potassium permeability in end-stage renal disease. *The Journal of Pathology*, *206*(1), 46–51. <https://doi.org/10.1002/path.1750>
- McDonel, J. L. (1974). In Vivo Effects of Clostridium perfringens Enteropathogenic Factors on the Rat Ileum. *Infection and Immunity*, *10*(5), 1156–62. Retrieved from <http://www.ncbi.nlm.nih.gov/pubmed/16558104>
- Neylon, C. B., Fowler, C. J., & Furness, J. B. (2006). Regulation of the slow afterhyperpolarization in enteric neurons by protein kinase A. *Autonomic Neuroscience: Basic and Clinical*. <https://doi.org/10.1016/j.autneu.2006.02.028>
- Neylon, C. B., Nurgali, K., Hunne, B., Robbins, H. L., Moore, S., Chen, M. X., & Furness, J. B. (2004). Intermediate-conductance calcium-activated potassium channels in enteric neurones of the mouse: pharmacological, molecular and immunochemical evidence for their role in mediating the slow afterhyperpolarization. *Journal of Neurochemistry*, *90*(6), 1414–1422. <https://doi.org/10.1111/j.1471-4159.2004.02593.x>
- Nguyen, T. V., Poole, D. P., Harvey, J. R., Stebbing, M. J., & Furness, J. B. (2005). Investigation of PKC isoform-specific translocation and targeting of the current of the late afterhyperpolarizing potential of myenteric AH neurons. *European Journal of Neuroscience*, *21*(4), 905–913. <https://doi.org/10.1111/j.1460-9568.2005.03931.x>
- Nguyen, T. V., Matsuyama, H., Baell, J., Hunne, B., Fowler, C. J., Smith, J. E., ... Furness, J. B. (2007). Effects of compounds that influence IK (KCNN4) channels on afterhyperpolarizing potentials, and determination of IK channel sequence, in guinea pig enteric neurons. *Journal of Neurophysiology*, *97*(3), 2024–31. <https://doi.org/10.1152/jn.00935.2006>

- Nicholls, J. G., Martin, A. R., Fuchs, P. A., Brown, D. A., Diamond, M. E., & Weisblat, D. A. (2012). *From neuron to brain* (5th ed.). Sunderland: Sinauer.
- North, R. A. (1973). The calcium-dependent slow after-hyperpolarization in myenteric plexus neurones with tetrodotoxin-resistant action potentials. *British Journal of Pharmacology*, *49*(4), 709–711. <https://doi.org/10.1111/j.1476-5381.1973.tb08550.x>
- Orio, P., Rojas, P., Ferreira, G., & Latorre, R. (2002). New disguises for an old channel: MaxiK channel beta-subunits. *News in Physiological Sciences : An International Journal of Physiology Produced Jointly by the International Union of Physiological Sciences and the American Physiological Society*, *17*, 156–61. Retrieved from <http://www.ncbi.nlm.nih.gov/pubmed/12136044>
- Pacheco Otalora, L. F., Hernandez, E. F., Arshadmansab, M. F., Francisco, S., Willis, M., Ermolinsky, B., ... Garrido-Sanabria, E. R. (2008). Down-regulation of BK channel expression in the pilocarpine model of temporal lobe epilepsy. *Brain Research*, *1200*, 116–131. <https://doi.org/10.1016/j.brainres.2008.01.017>
- Pan, H., & Gershon, M. D. (2000). Activation of Intrinsic Afferent Pathways in Submucosal Ganglia of the Guinea Pig Small Intestine. *Journal of Neuroscience*, *20*(9).
- Quirk, J. C., & Reinhart, P. H. (2001). Identification of a novel tetramerization domain in large conductance KCa channels. *Neuron*, *32*(1), 13–23. [https://doi.org/10.1016/S0896-6273\(01\)00444-5](https://doi.org/10.1016/S0896-6273(01)00444-5)
- Rundén-Pran, E., Haug, F. M., Storm, J. F., & Ottersen, O. P. (2002). BK channel activity determines the extent of cell degeneration after oxygen and glucose deprivation: a study in organotypical hippocampal slice cultures. *Neuroscience*, *112*(2), 277–288. [https://doi.org/10.1016/S0306-4522\(02\)00092-1](https://doi.org/10.1016/S0306-4522(02)00092-1)
- Rüttiger, L., Sausbier, M., Zimmermann, U., Winter, H., Braig, C., Engel, J., ... Knipper, M. (2004). Deletion of the Ca²⁺-activated potassium (BK) alpha-subunit but not the BKbeta1-subunit leads to progressive hearing loss. *Proceedings of the National Academy of Sciences of the United States of America*, *101*(35), 12922–7. <https://doi.org/10.1073/pnas.0402660101>
- Salkoff, L., Butler, A., Ferreira, G., Santi, C., & Wei, A. (2006). High-conductance potassium channels of the SLO family. *Nature Reviews Neuroscience*, *7*(12), 921–931. <https://doi.org/10.1038/nrn1992>
- Sandle, G. I., & Hunter, M. (2010). Apical potassium (BK) channels and enhanced potassium secretion in human colon. *QJM*, *103*(2).
- Sausbier, M., Hu, H., Arntz, C., Feil, S., Kamm, S., Adelsberger, H., ... Ruth, P. (2004). Cerebellar ataxia and Purkinje cell dysfunction caused by Ca²⁺-activated K⁺ channel deficiency. *Proceedings of the National Academy of Sciences of the United States of America*, *101*(25), 9474–8. <https://doi.org/10.1073/pnas.0401702101>
- Sausbier, M., Matos, J. E., Sausbier, U., Beranek, G., Arntz, C., Neuhuber, W., ... Leipziger, J. (2006). Distal colonic K(+) secretion occurs via BK channels. *Journal of the American Society of Nephrology : JASN*, *17*(5), 1275–82. <https://doi.org/10.1681/ASN.2005101111>

- Schreiber, M., Wei, A., Yuan, A., Gaut, J., Saito, M., & Salkoff, L. (1998). Slo3, a novel pH-sensitive K⁺ channel from mammalian spermatocytes. *Journal of Biological Chemistry*, 273(6), 3509–3516. <https://doi.org/10.1074/jbc.273.6.3509>
- Stefani, E., Ottolia, M., Noceti, F., Olcese, R., Wallner, M., Latorre, R., & Toro, L. (1997). Voltage-controlled gating in a large conductance Ca²⁺-sensitive K⁺ channel (hslo). *Proceedings of the National Academy of Sciences of the United States of America*, 94(10), 5427–31. Retrieved from <http://www.ncbi.nlm.nih.gov/pubmed/9144254>
- Tsantoulas, C., & McMahon, S. B. (2014). Opening paths to novel analgesics: the role of potassium channels in chronic pain. *Trends in Neurosciences*, 37(3), 146–158. <https://doi.org/10.1016/j.tins.2013.12.002>
- Typlt, M., Mirkowski, M., Azzopardi, E., Ruettiger, L., Ruth, P., Schmid, S., ... Hikosaka, O. (2013). Mice with Deficient BK Channel Function Show Impaired Prepulse Inhibition and Spatial Learning, but Normal Working and Spatial Reference Memory. *PLoS ONE*, 8(11), e81270. <http://doi.org/10.1371/journal.pone.0081270>
- Vogalis, F., Furness, J. B., & Kunze, W. A. A. (2001). Afterhyperpolarization Current in Myenteric Neurons of the Guinea Pig Duodenum. *Journal of Neurophysiology*, 85(5). Retrieved from <http://jn.physiology.org/content/85/5/1941.short>
- Vogalis, F., Harvey, J. R., & Furness, J. B. (2003). PKA-mediated inhibition of a novel K⁺ channel underlies the slow after-hyperpolarization in enteric AH neurons. *The Journal of Physiology*, 548(3), 801–814. <https://doi.org/10.1111/j..2003.t01-1-00801.x>
- Wallner, M., Meera, P., & Toro, L. (1996). Determinant for beta-subunit regulation in high-conductance voltage-activated and Ca(2+)-sensitive K⁺ channels: an additional transmembrane region at the N terminus. *Proceedings of the National Academy of Sciences of the United States of America*, 93(25), 14922–14927. <https://doi.org/10.1073/pnas.93.25.14922>
- Wood, J. D., & Kirchgessner, A. (2004). Slow excitatory metabotropic signal transmission in the enteric nervous system. *Neurogastroenterology and Motility*, 16(SUPPL. 1), 71–80. <https://doi.org/10.1111/j.1743-3150.2004.00479.x>
- Zhang, X.-F., Gopalakrishnan, M., & Shieh, C.-C. (2003). Modulation of action potential firing by iberiotoxin and NS1619 in rat dorsal root ganglion neurons. *Neuroscience*, 122(4), 1003–1011. <https://doi.org/10.1016/j.neuroscience.2003.08.035>